



The Continuous Adjoint Method for Multi-Fidelity Hypersonic Inlet Design

Heather L. Kline

Research Advisor: Professor Juan Alonso

Stanford University

AMS Seminar

NASA Ames Research Center

March 23rd, 2017



Introduction

Background &
Literature Review

Methodology

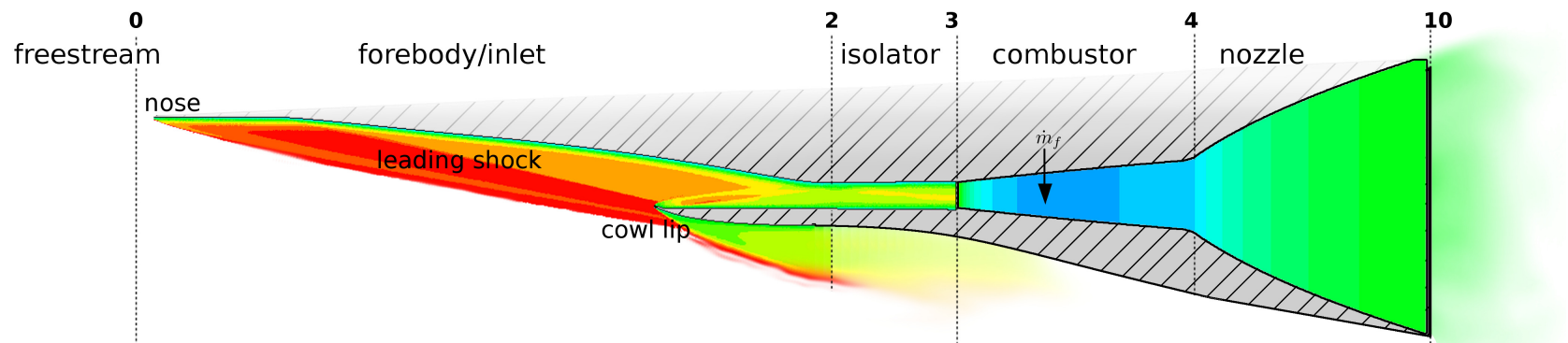
Results

Conclusions &
Future Work

Publications

References

Supersonic Combustion Ramjets (scramjets) are a potentially efficient propulsion system for access to space, but many challenges remain which motivate using simulation-based design.





Introduction

Background & Literature Review

Methodology

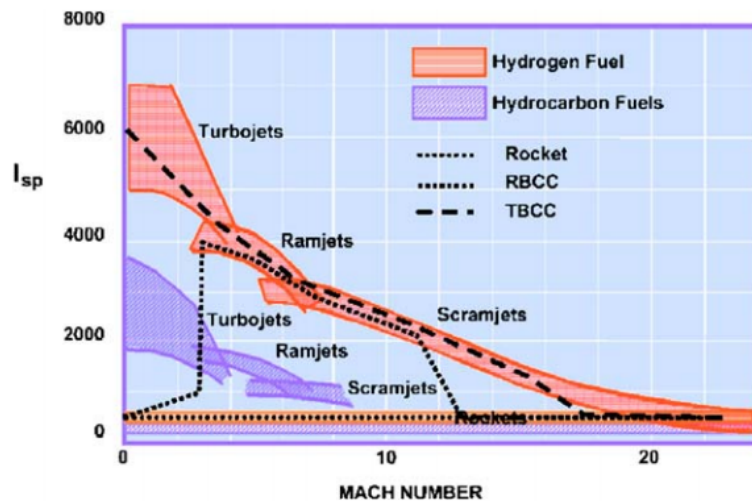
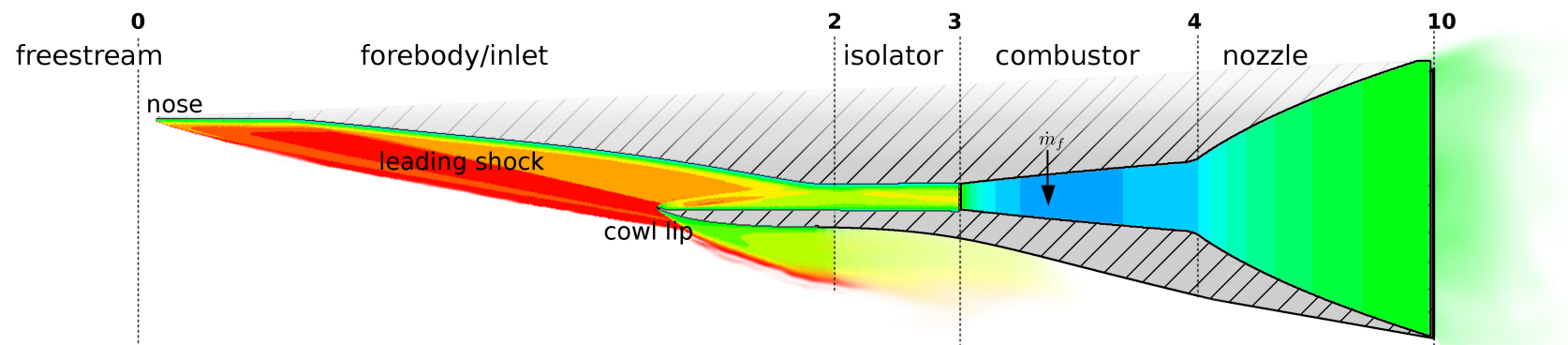
Results

Conclusions & Future Work

Publications

References

Supersonic Combustion Ramjets (scramjets) are a potentially efficient propulsion system for access to space, but many challenges remain which motivate using simulation-based design.



P. Moses et al. (2004). "NASA Hypersonic Flight Demonstrators—Overview, Status, and Future Plans". In: *Acta Astronautica* 55.3, pp. 619–630



Introduction

Background & Literature Review

Methodology

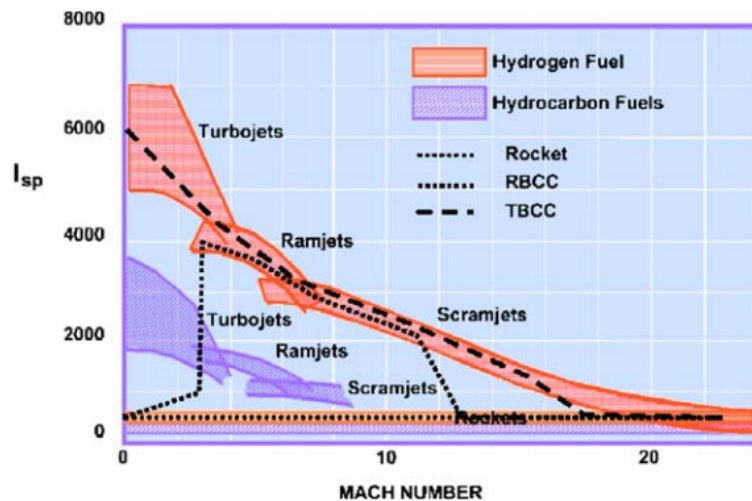
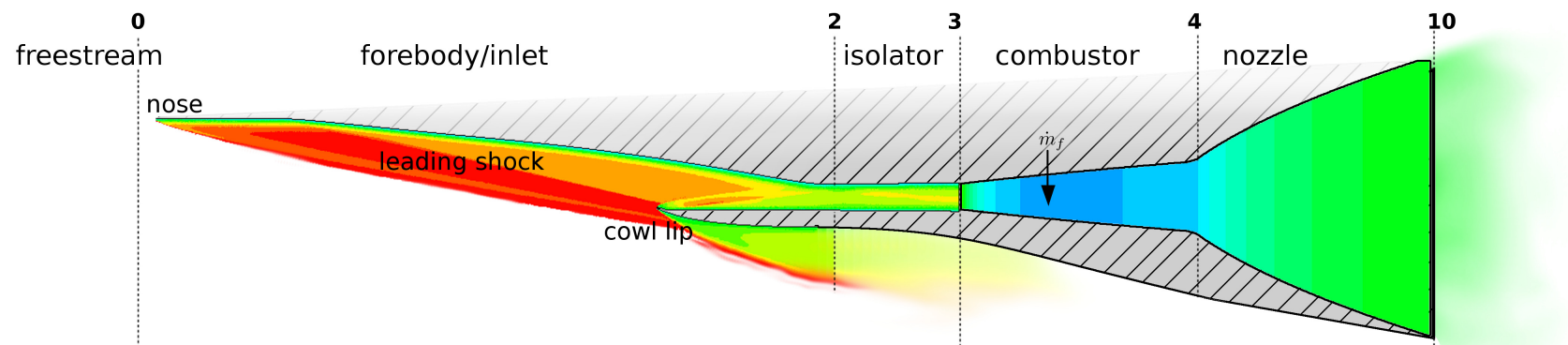
Results

Conclusions & Future Work

Publications

References

Supersonic Combustion Ramjets (scramjets) are a potentially efficient propulsion system for access to space, but many challenges remain which motivate using simulation-based design.



X-43A Artist's Conception. Image credit: NASA

P. Moses et al. (2004). "NASA Hypersonic Flight Demonstrators—Overview, Status, and Future Plans". In: *Acta Astronautica* 55.3, pp. 619–630



Scramjet Design Process

Background &
Literature Review

Methodology

Results

Conclusions &
Future Work

Publications

References

- Low fidelity initial design included the full flow path, and provides sizing and parameters such as a compression ratio.¹
- Simulation-based design and detailed analysis of isolated components.^{2,3,4}
- Components incrementally tested and combined.⁵

¹M. Smart (2012). "How Much Compression Should a Scramjet Inlet Do?" In: [AIAA Journal](#) 50.3, pp. 610–619.

²R. Gollan and P. Ferlemann (2011). "Investigation of REST-class Hypersonic Inlet Designs". In: [17th AIAA International Space Planes and Hypersonic Systems and Technologies Conference](#).

³C. Tarn and R. Baurle (2001). "Inviscid CFD Analysis of Streamline Traced Hypersonic Inlets at Off-Design Conditions". In: [39th Aerospace Sciences Meeting and Exhibit, Reno, NV](#).

⁴W. Huang et al. (2011). "Flow-field analysis of a typical hydrogen-fueled dual-mode scramjet combustor". In: [Journal of Aerospace Engineering](#) 25.3, pp. 336–346.

⁵K. Jackson, M. Gruber, and S. Buccellato (2011). "HIFiRE Flight 2 Overview and Status Update 2011". In: [17th AIAA International Space Planes and Hypersonic Systems and Technologies Conference](#), pp. 2011–2202.



Challenges

Background &
Literature Review

Methodology

Results

Conclusions &
Future Work

Publications

References



Mach 7 wind tunnel test of the full-scale X-43A model in NASA Langley's 8-Foot High Temperature Tunnel.



Challenges

Background &
Literature Review

Methodology

Results

Conclusions &
Future Work

Publications

References

- Low-fidelity analysis of the full flowpath provides limited detail.
- High fidelity simulations of isolated components neglect flowpath performance.



Mach 7 wind tunnel test of the full-scale X-43A model in NASA Langley's 8-Foot High Temperature Tunnel.



Challenges

Background &
Literature Review

Methodology

Results

Conclusions &
Future Work

Publications

References

- Low-fidelity analysis of the full flowpath provides limited detail.
- High fidelity simulations of isolated components neglect flowpath performance.
- Many interacting and competing factors influence performance.



Mach 7 wind tunnel test of the full-scale X-43A model in NASA Langley's 8-Foot High Temperature Tunnel.



Challenges

Background &
Literature Review

Methodology

Results

Conclusions &
Future Work

Publications

References

- Low-fidelity analysis of the full flowpath provides limited detail.
- High fidelity simulations of isolated components neglect flowpath performance.
- Many interacting and competing factors influence performance.
- Gradient-based optimization is a useful tool, but the more efficient methods of calculating gradients do not provide all the relevant performance metrics.



Mach 7 wind tunnel test of the full-scale X-43A model in NASA Langley's 8-Foot High Temperature Tunnel.



Contributions

Background &
Literature Review

Methodology

Results

Conclusions &
Future Work

Publications

References



Contributions

Background &
Literature Review

Methodology

Results

Conclusions &
Future Work

Publications

References

- A new generalized adjoint functional which facilitates **flexible outflow-based functionals**, including those that use **external models**.



Contributions

Background &
Literature Review

Methodology

Results

Conclusions &
Future Work

Publications

References

- A new generalized adjoint functional which facilitates **flexible outflow-based functionals**, including those that use **external models**. → enables multi-fidelity integrated flowpath design.



Contributions

Background &
Literature Review

Methodology

Results

Conclusions &
Future Work

Publications

References

- A new generalized adjoint functional which facilitates **flexible outflow-based functionals**, including those that use **external models**. → enables multi-fidelity integrated flowpath design.
- A **multi-objective adjoint** implemented by using superposition of boundary conditions.



Contributions

Background &
Literature Review

Methodology

Results

Conclusions &
Future Work

Publications

References

- A new generalized adjoint functional which facilitates **flexible outflow-based functionals**, including those that use **external models**. → enables multi-fidelity integrated flowpath design.
- A **multi-objective adjoint** implemented by using superposition of boundary conditions. → addresses competing objectives.



Contributions

Background &
Literature Review

Methodology

Results

Conclusions &
Future Work

Publications

References

- A new generalized adjoint functional which facilitates **flexible outflow-based functionals**, including those that use **external models**. → enables multi-fidelity integrated flowpath design.
- A **multi-objective adjoint** implemented by using superposition of boundary conditions. → addresses competing objectives.
- These methods have been implemented and utilized for multi-objective and multi-fidelity shape optimization of a hypersonic inlet.



Contributions

Background &
Literature Review

Methodology

Results

Conclusions &
Future Work

Publications

References

- A new generalized adjoint functional which facilitates **flexible outflow-based functionals**, including those that use **external models**. → enables multi-fidelity integrated flowpath design.
- A **multi-objective adjoint** implemented by using superposition of boundary conditions. → addresses competing objectives.
- These methods have been implemented and utilized for multi-objective and multi-fidelity shape optimization of a hypersonic inlet.
- Results show large performance changes for small geometry modifications, and interesting relationships between competing objectives.



Table of Contents

Background &
Literature Review

Methodology

Results

Conclusions &
Future Work

Publications

References

- 1 Background & Literature Review
- 2 Methodology
- 3 Results
- 4 Conclusions & Future Work



Table of Contents

Background &
Literature Review

Methodology

Results

Conclusions &
Future Work

Publications

References

- 1 Background & Literature Review
 - Hypersonic Effects
 - Design Quantities of Interest
 - Optimization
 - The Continuous Adjoint Method

2 Methodology

3 Results

4 Conclusions & Future Work



Hypersonic Effects

Background & Literature Review

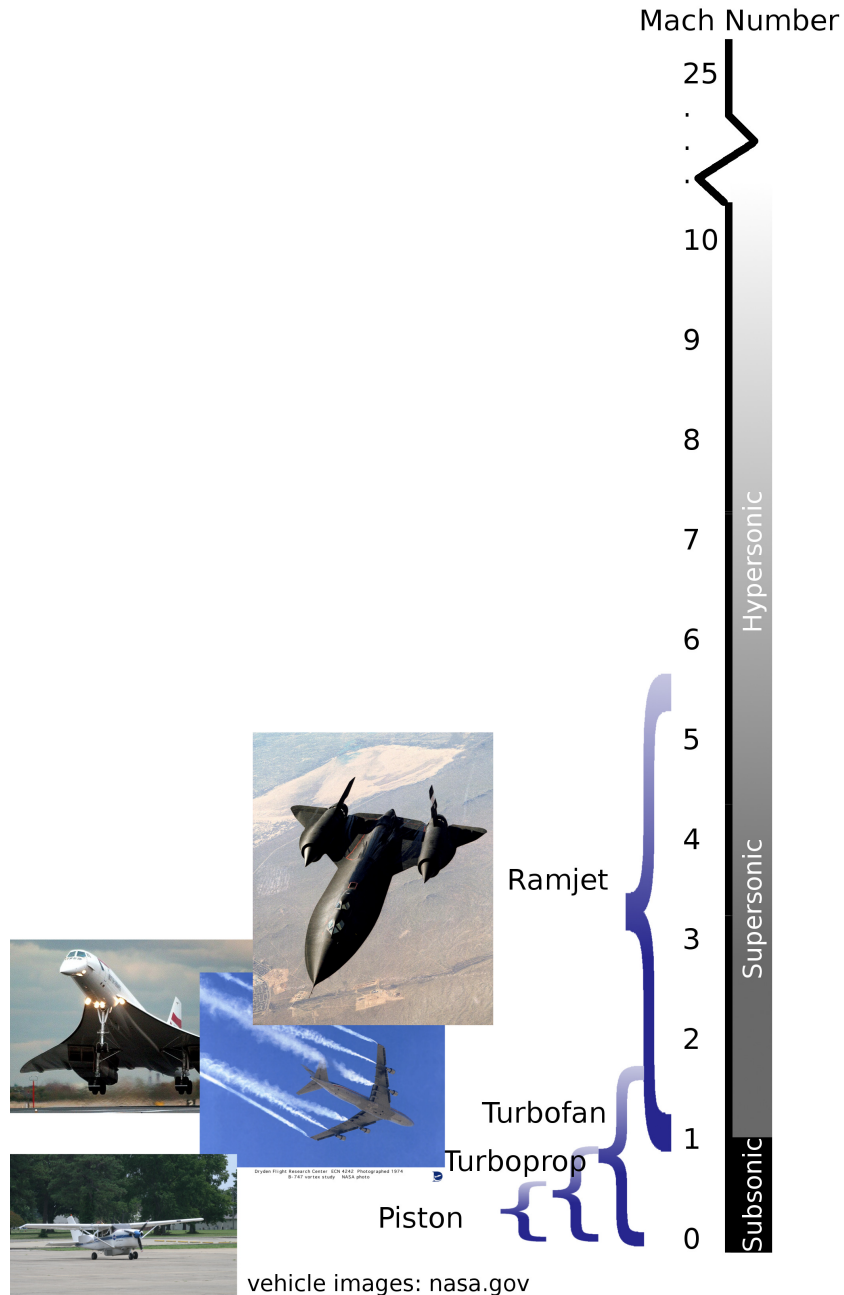
Methodology

Results

Conclusions & Future Work

Publications

References





Hypersonic Effects

Background &
Literature Review

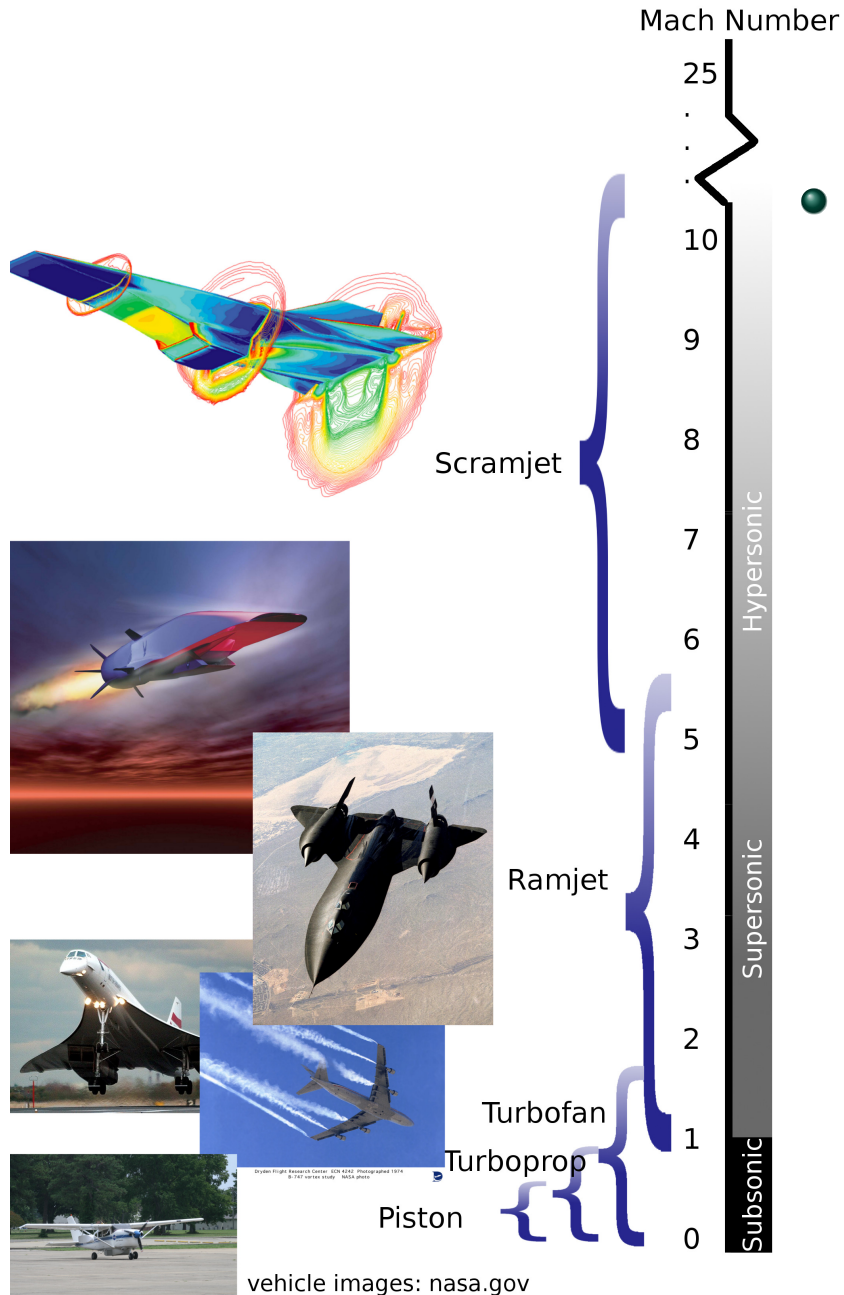
Methodology

Results

Conclusions &
Future Work

Publications

References



- A collection of phenomena become more significant above \approx Mach 5:



Hypersonic Effects

Background &
Literature Review

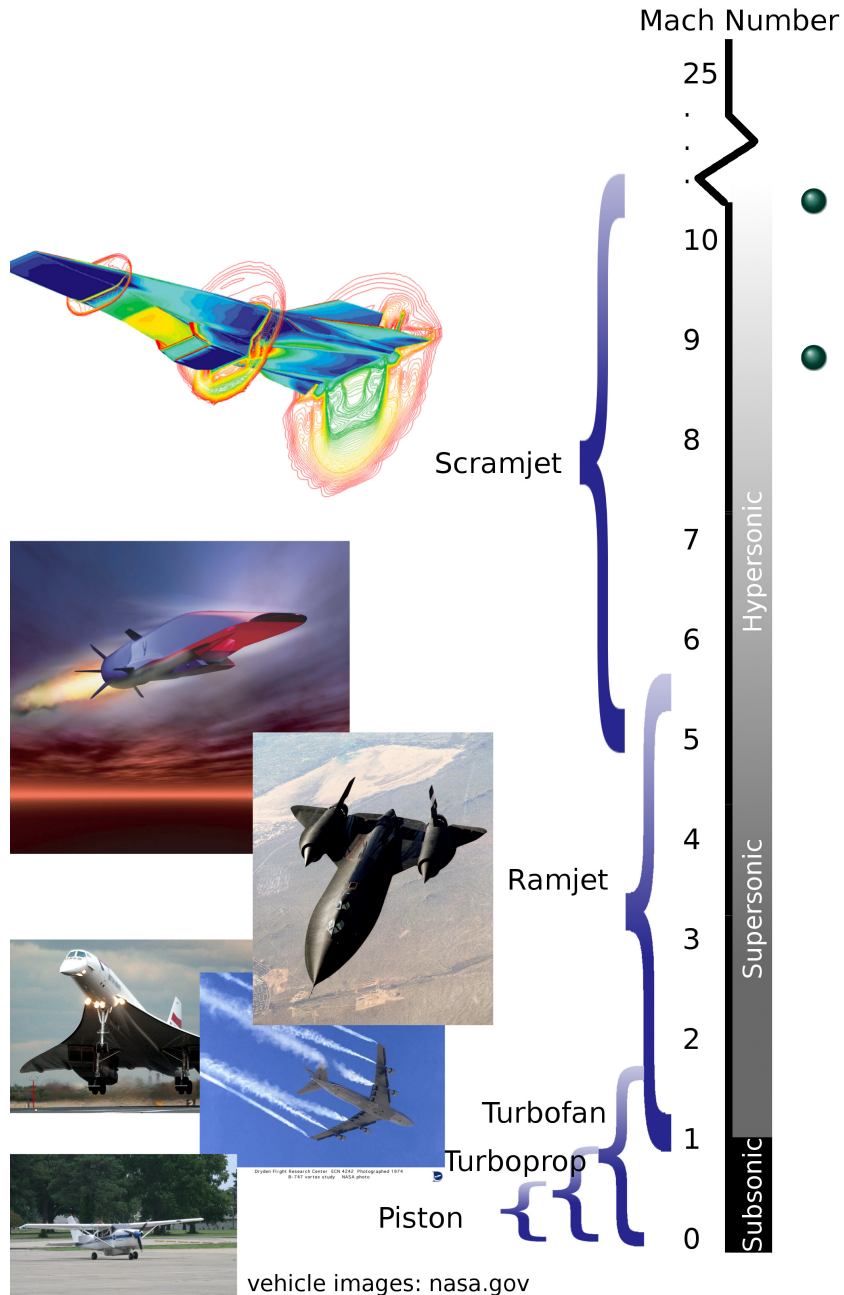
Methodology

Results

Conclusions &
Future Work

Publications

References



- A collection of phenomena become more significant above \approx Mach 5:
- Thin shock layers, entropy layers, viscous interaction become more significant with increased Mach and temperature.



Hypersonic Effects

Background & Literature Review

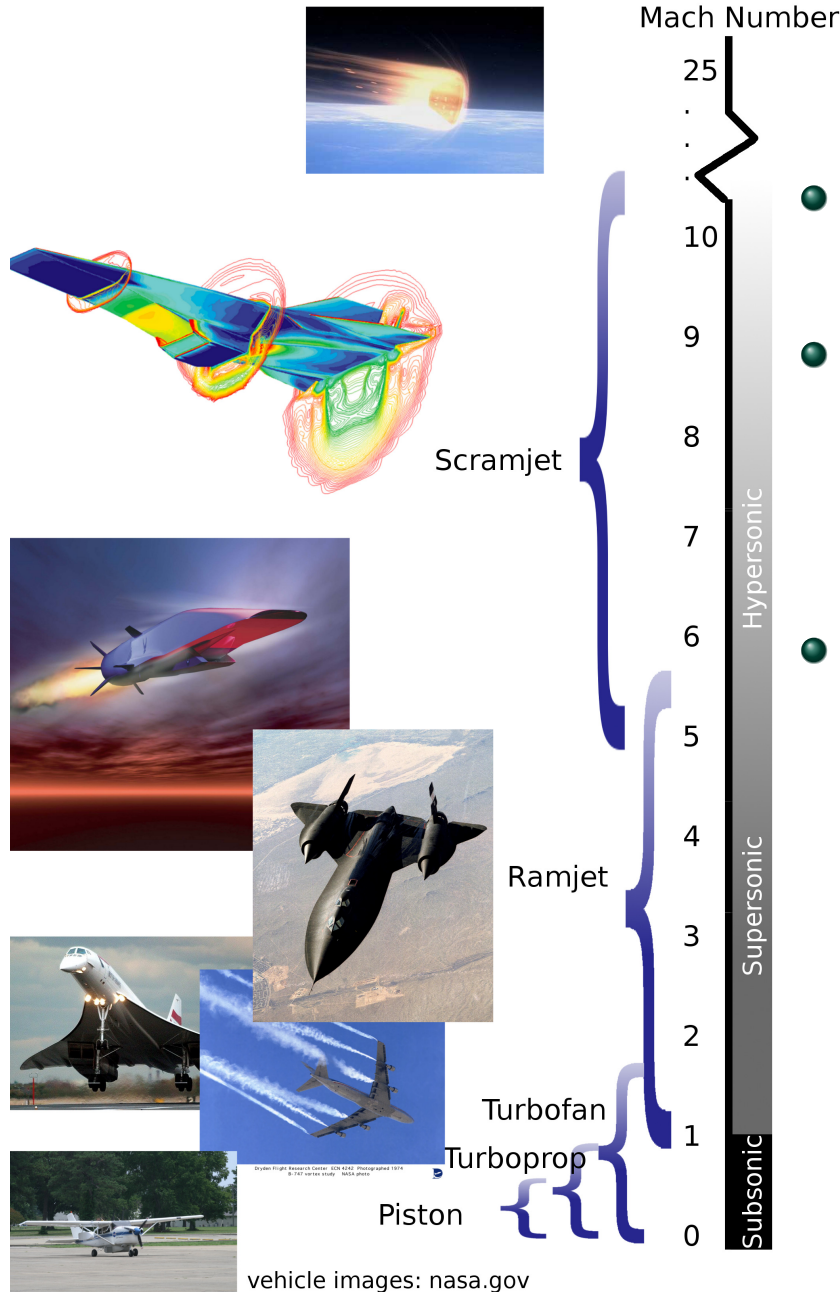
Methodology

Results

Conclusions & Future Work

Publications

References



- A collection of phenomena become more significant above \approx Mach 5:
- Thin shock layers, entropy layers, viscous interaction become more significant with increased Mach and temperature.
- As temperature increases, real gas effects ($T \gtrsim 800^\circ\text{K}$), chemical reactions ($T \gtrsim 2,000^\circ\text{K}$), ionized flow ($T \gtrsim 9,000^\circ\text{K}$), and radiative heat flux ($T \gtrsim 10,000^\circ\text{K}$) become significant.



Hypersonic Effects

Background &
Literature Review

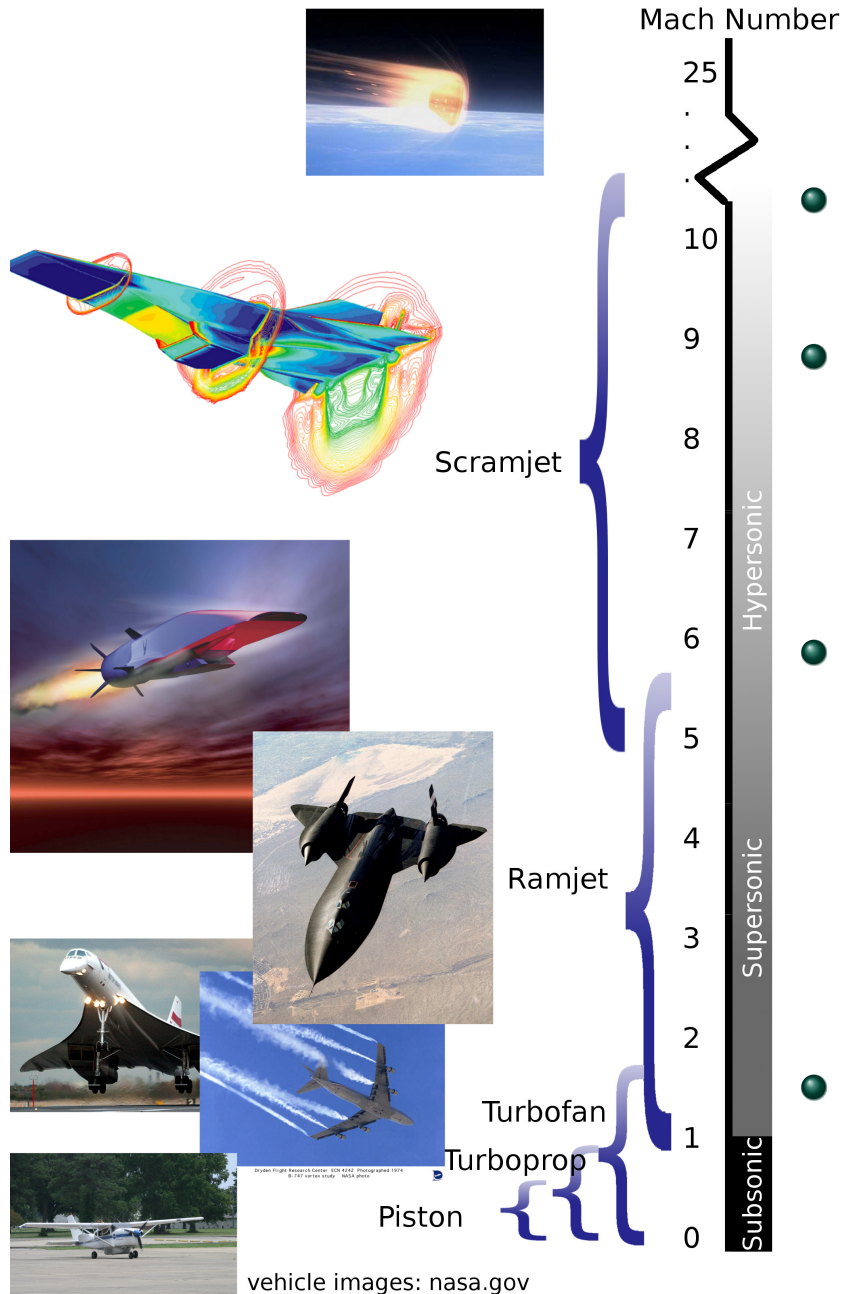
Methodology

Results

Conclusions &
Future Work

Publications

References



- A collection of phenomena become more significant above \approx Mach 5:
- Thin shock layers, entropy layers, viscous interaction become more significant with increased Mach and temperature.
- As temperature increases, real gas effects ($T \gtrsim 800^\circ\text{K}$), chemical reactions ($T \gtrsim 2,000^\circ\text{K}$), ionized flow ($T \gtrsim 9,000^\circ\text{K}$), and radiative heat flux ($T \gtrsim 10,000^\circ\text{K}$) become significant.
- Above ≈ 92 km rarefied gas effects become significant.



Hypersonic Effects

Background & Literature Review

Methodology

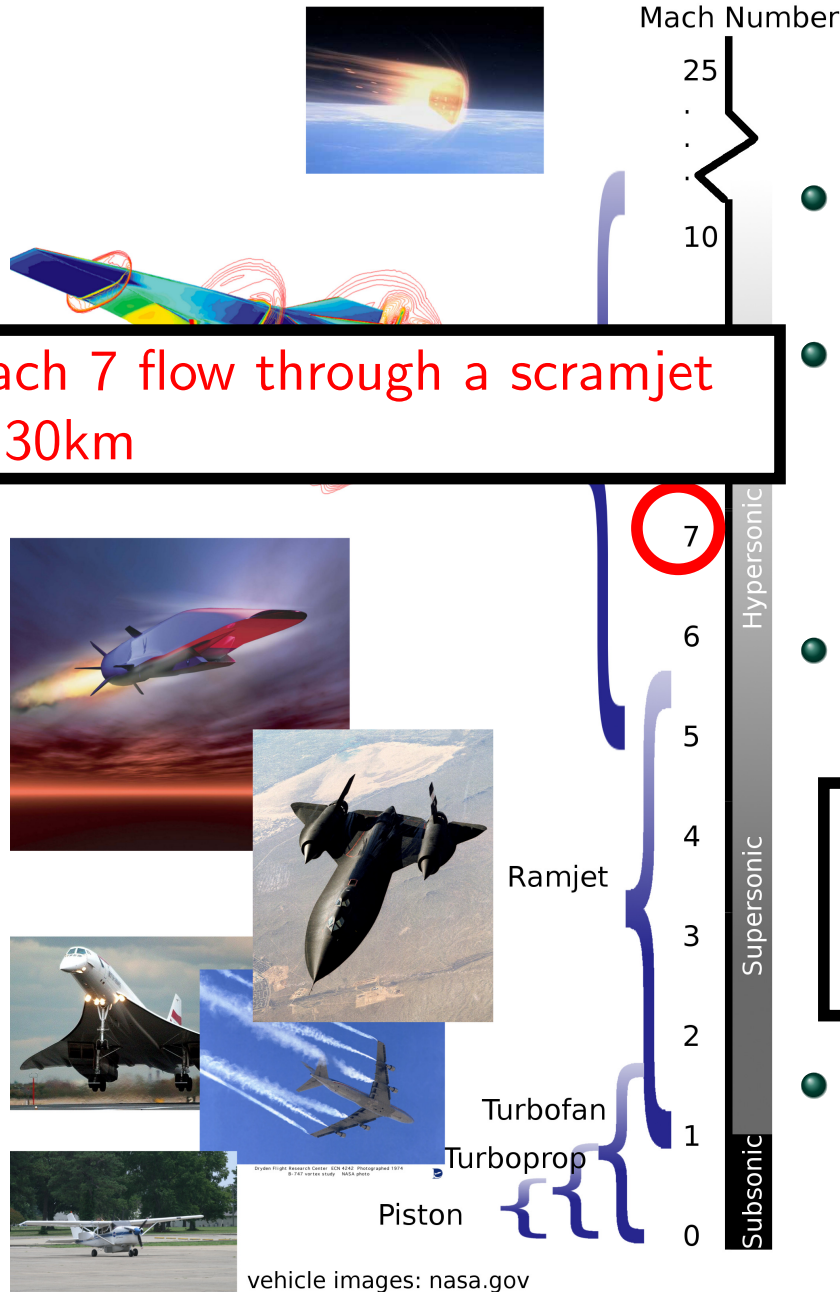
Results

Conclusions & Future Work

Publications

References

Mach 7 flow through a scramjet at 30km



- A collection of phenomena become more significant above \approx Mach 5:
- **Thin shock layers, entropy layers, viscous interaction** become more significant with increased Mach and temperature.
- As temperature increases, **real gas effects** ($T \gtrsim 800^\circ\text{K}$), **changing specific heats** ($T \gtrsim 2,000^\circ\text{K}$), **changing specific heats included in 1D flow model of combustor/nozzle.**
- Above ≈ 92 km rarefied gas effects become significant.



Design Quantities of Interest

Background & Literature Review

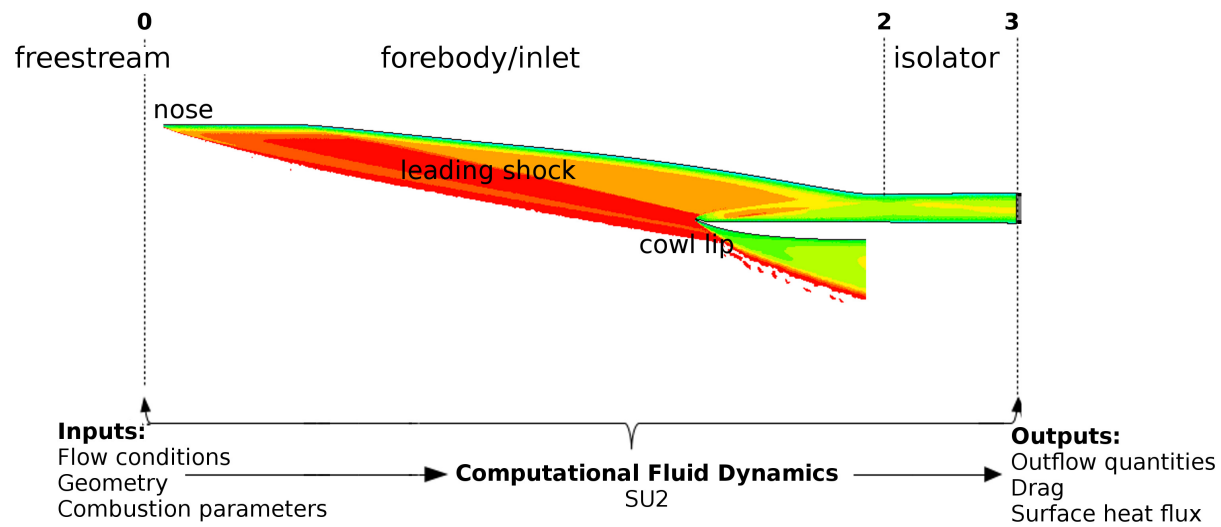
Methodology

Results

Conclusions & Future Work

Publications

References





Design Quantities of Interest

Background &
Literature Review

Methodology

Results

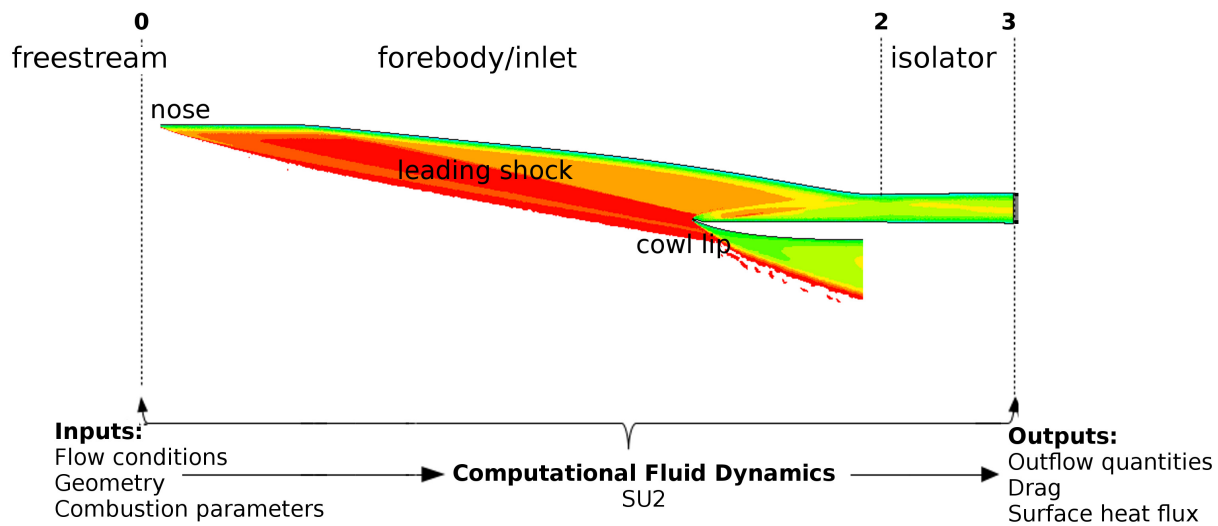
Conclusions &
Future Work

Publications

References

$$\text{Total pressure ratio: } P_{tr} = \frac{P_{t3}}{P_{t0}}$$

$$\text{Surface heat flux: } \int_S -k \nabla T \cdot \vec{n} ds$$





Design Quantities of Interest

Background & Literature Review

Methodology

Results

Conclusions & Future Work

Publications

References

Total pressure ratio: $P_{tr} = \frac{P_{t3}}{P_{t0}}$

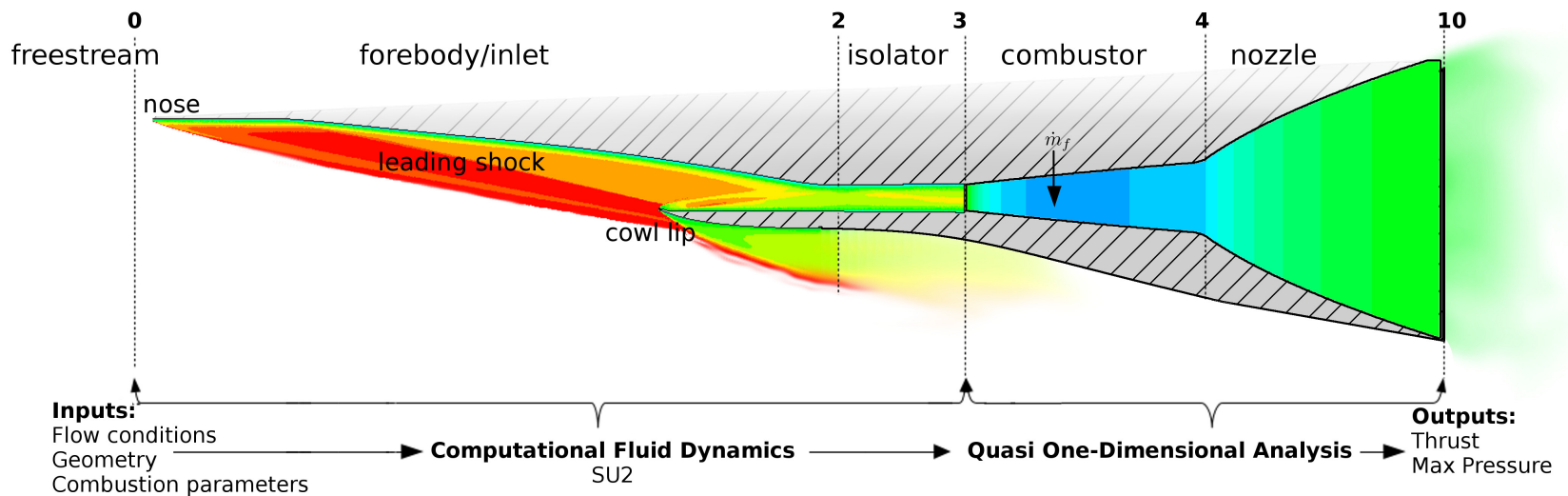
Surface heat flux: $\int_S -k \nabla T \cdot \vec{n} ds$

Thrust: $\mathcal{F}_{un} = \dot{m}_0 c_0 M_0 \left((1 + f) \frac{M_{10}}{M_0} \sqrt{\frac{T_{10}}{T_0}} - 1 \right) + \frac{\mathcal{A}_{10}}{\mathcal{A}_0} \left(\frac{P_{10}}{P_0} - 1 \right)$

Specific installed thrust: $\frac{\mathcal{F}_{un} - D_{est}}{\dot{m}}$

Total temperature ratio (relates to unstart): $\tau = \frac{T_{te}}{T_{t0}}$

Combustor maximum pressure (relates to structural limits): P_{max} .





Design Quantities of Interest

Background & Literature Review

Methodology

Results

Conclusions & Future Work

Publications

References

Total pressure ratio: $P_{tr} = \frac{P_{t3}}{P_{t0}}$

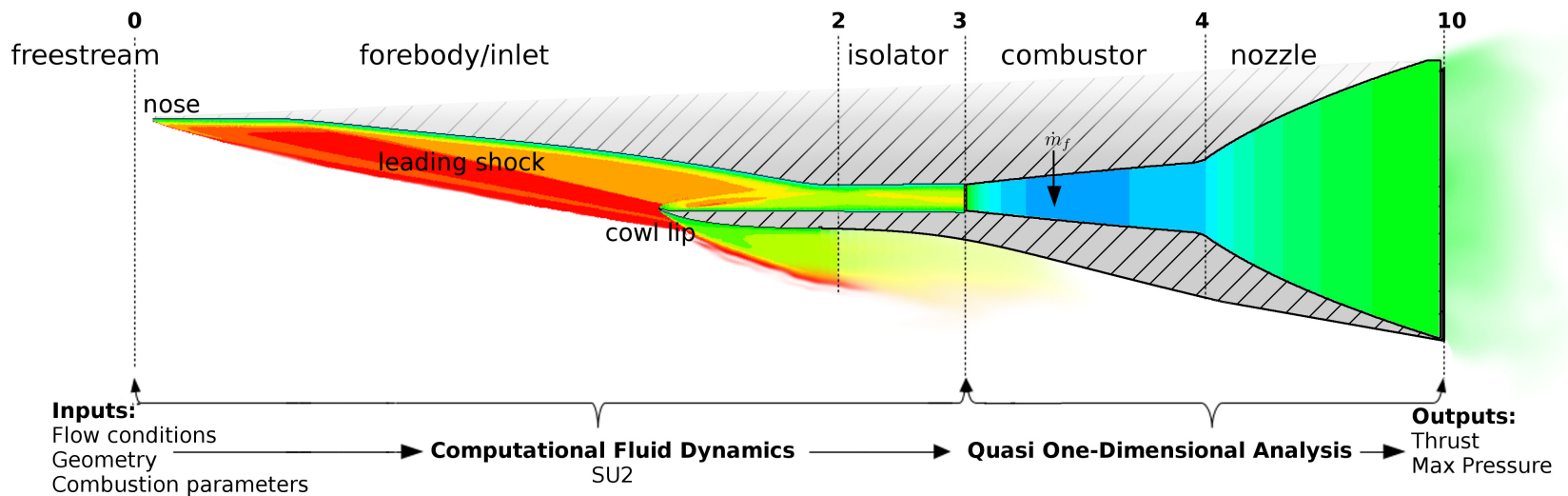
Surface heat flux: $\int_S -k \nabla T \cdot \vec{n} ds$

Thrust: $\mathcal{F}_{un} = \dot{m}_0 c_0 M_0 \left((1 + f) \frac{M_{10}}{M_0} \sqrt{\frac{T_{10}}{T_0}} - 1 \right) + \frac{\mathcal{A}_{10}}{\mathcal{A}_0} \left(\frac{P_{10}}{P_0} - 1 \right)$

Specific installed thrust: $\frac{\mathcal{F}_{un} - D_{est}}{\dot{m}}$

Total temperature ratio (relates to unstart): $\tau = \frac{T_{te}}{T_{t0}}$

Combustor maximum pressure (relates to structural limits): P_{max} .





Optimization

Background &
Literature Review

Methodology

Results

Conclusions &
Future Work

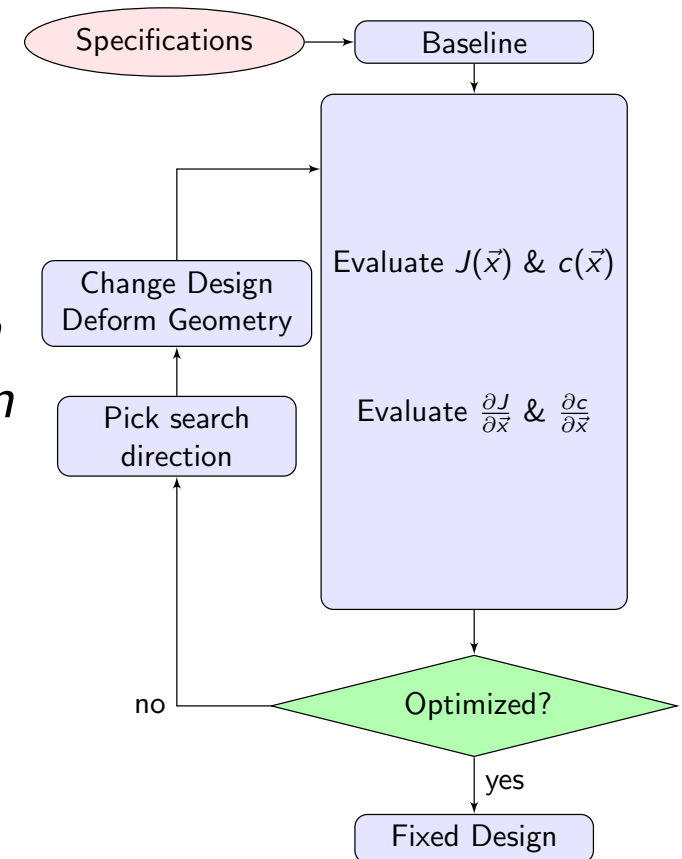
Publications

References

Non-Linear Program:

$$\begin{aligned} &\text{minimize} && J(\vec{x}) \\ &\text{with respect to} && \vec{x} \in \mathbb{R}^n \\ &\text{subject to} && \hat{c}_j(\vec{x}) = 0, \quad j = 1, \dots, \hat{m} \\ & && c_k(\vec{x}) \geq 0, \quad k = 1, \dots, m \end{aligned}$$

Optimization algorithms have been developed by (Powell 1978), (Wilson 1963), (Boggs and Tolle 1995) and others. The SNOPT (Gill, Murray, and Saunders 2006) algorithm is used in this work.





The Continuous Adjoint Method

Background &
Literature Review

Methodology

Results

Conclusions &
Future Work

Publications

References

- Cost \approx function, independent to # design variables.
- Derive new PDE for new functionals.
- Sensitivity of one objective at a time.
- Limited to integral functions defined within the CFD volume.



The Continuous Adjoint Method

Background & Literature Review

Methodology

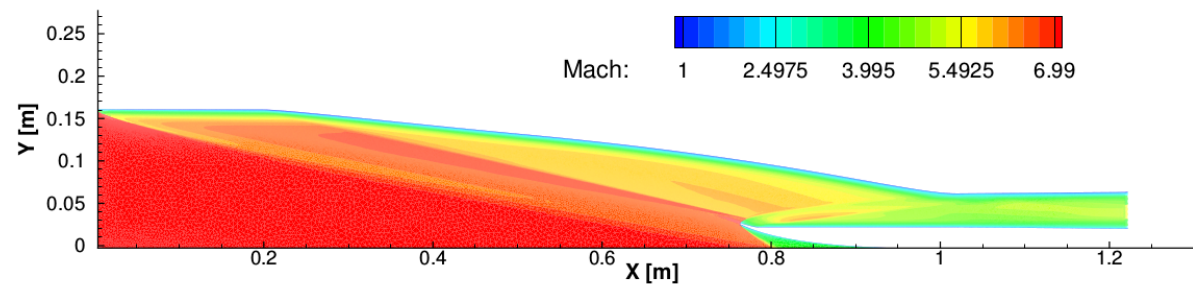
Results

Conclusions & Future Work

Publications

References

- Cost \approx function, independent to # design variables.
- Derive new PDE for new functionals.
- Sensitivity of one objective at a time.
- Limited to integral functions defined within the CFD volume.



Mach 7 flow through 2D scramjet inlet.



The Continuous Adjoint Method

Background &
Literature Review

Methodology

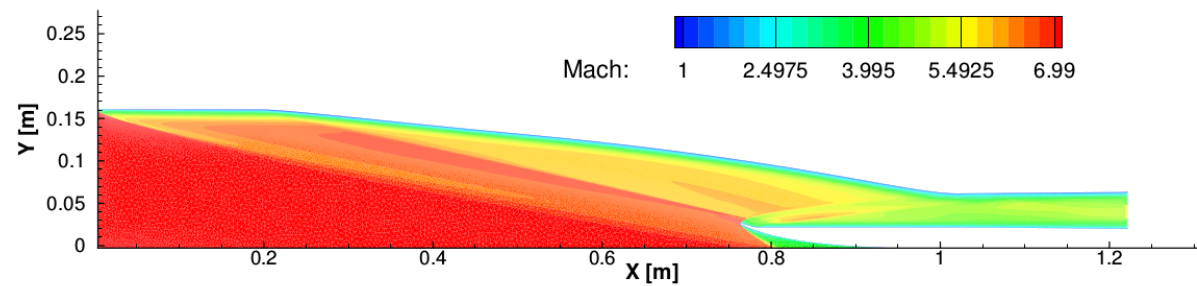
Results

Conclusions &
Future Work

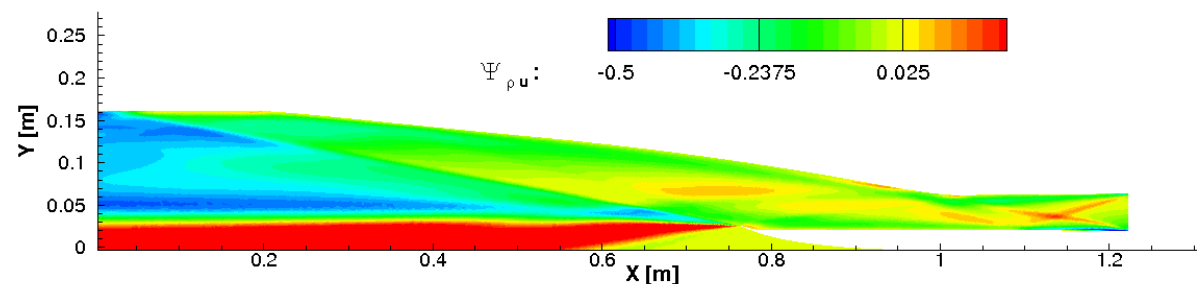
Publications

References

- Cost \approx function, independent to # design variables.
- Derive new PDE for new functionals.
- Sensitivity of one objective at a time.
- Limited to integral functions defined within the CFD volume.



Mach 7 flow through 2D scramjet inlet.



Adjoint of specific installed thrust.



The Continuous Adjoint Method

Background &
Literature Review

Methodology

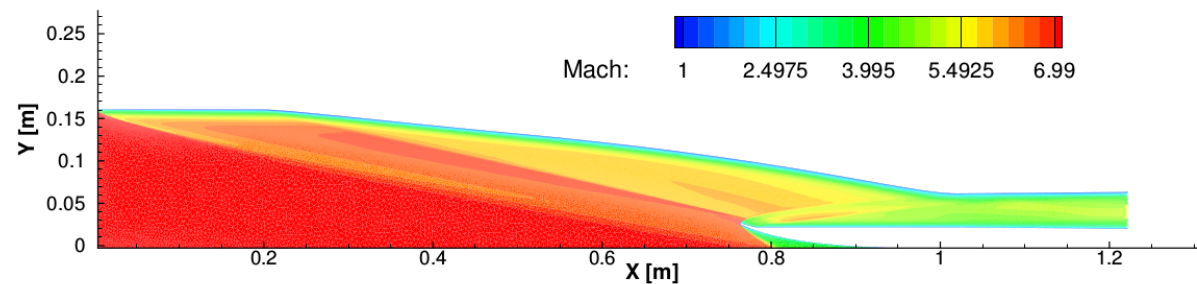
Results

Conclusions &
Future Work

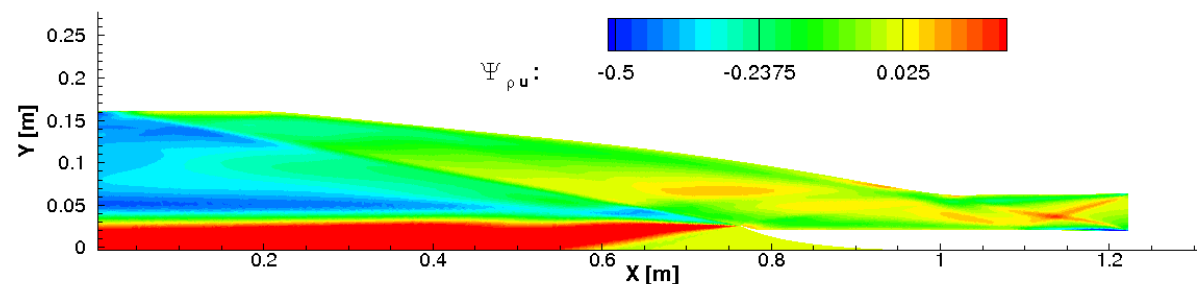
Publications

References

- Cost \approx function, independent to # design variables.
- Derive new PDE for new functionals. **Except on outflow boundaries.**
- Sensitivity of one objective at a time.
- Limited to integral functions defined within the CFD volume.



Mach 7 flow through 2D scramjet inlet.



Adjoint of specific installed thrust.



The Continuous Adjoint Method

Background & Literature Review

Methodology

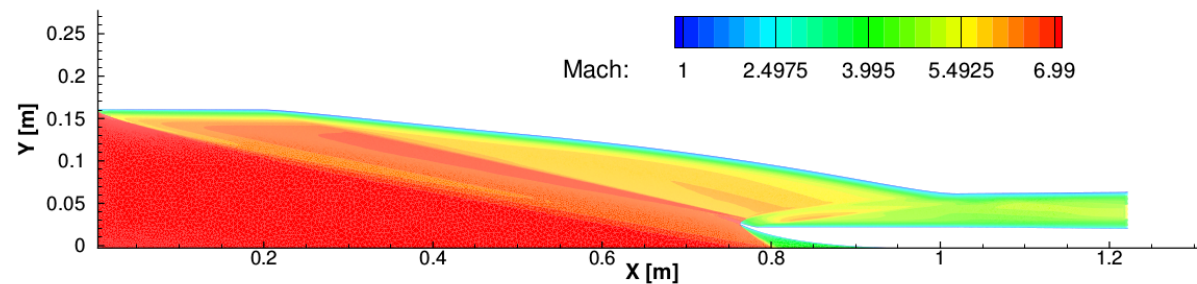
Results

Conclusions & Future Work

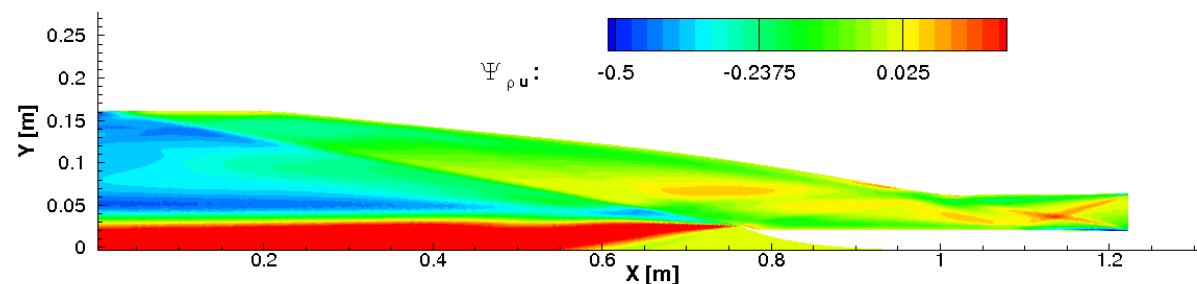
Publications

References

- Cost \approx function, independent to # design variables.
- Derive new PDE for new functionals. Except on outflow boundaries.
- Sensitivity of one objective at a time.
- Limited to integral functions defined within the CFD volume.



Mach 7 flow through 2D scramjet inlet.



Adjoint of specific installed thrust.



The Continuous Adjoint Method

Background &
Literature Review

Methodology

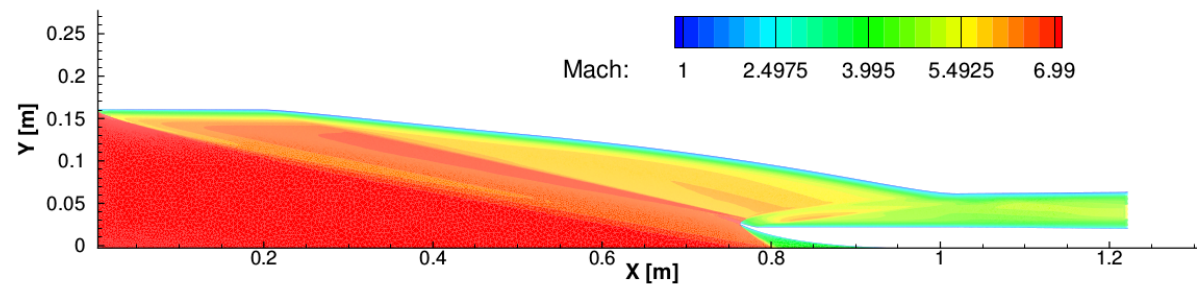
Results

Conclusions &
Future Work

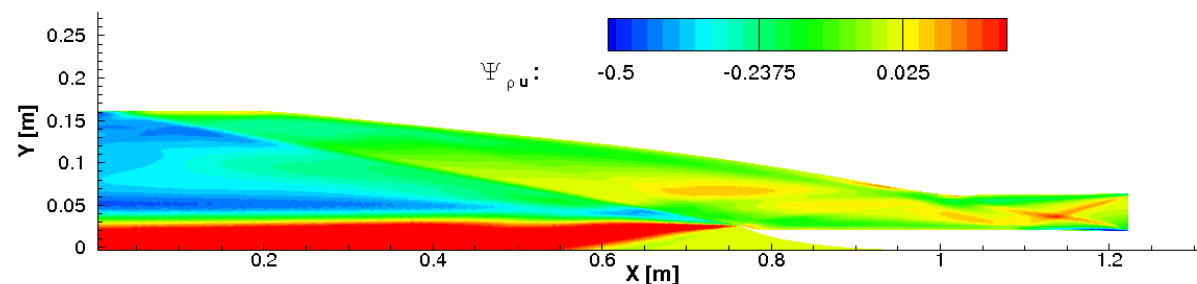
Publications

References

- Cost \approx function, independent to # design variables.
- Derive new PDE for new functionals. Except on outflow boundaries.
- Sensitivity of one objective at a time.
- Limited to integral functions defined within the CFD volume.



Mach 7 flow through 2D scramjet inlet.



Adjoint of specific installed thrust.



The Continuous Adjoint Method: Literature Review

Background &
Literature Review

Methodology

Results

Conclusions &
Future Work

Publications

References

- Optimal control of PDE systems by (Lions 1971) and (Pironneau 1984).
- Developed for aerodynamic optimization by (Jameson 1988).
- (Giles and Pierce 1997) and others provide the adjoint formulation for many objective functions defined on solid walls; (Hayashi, Ceze, and Volpe 2012) made developments in characteristic-based boundary conditions. (Arian and Salas 1999) studied admissible objectives on solid wall boundaries
- (Castro et al. 2007) developed the continuous adjoint for unstructured grids using a surface formulation.
- Previously available objectives on outflow boundaries limited to functions of pressure or total pressure provided by (Papadimitriou and Giannakoglou 2007), and functions of velocity in incompressible flow such as (Othmer 2008).



The Adjoint Method

Background &
Literature Review

Methodology

Results

Conclusions &
Future Work

Publications

References

A.k.a.: Lagrange multipliers, co-state problem, or dual problem.

J : Function of interest. R : Governing equations.

U : State variables (ex: conservative variables).

S : Design variables/independent variables (ex: surface shape).

$$J(U, S) \quad \frac{\delta J}{\delta S} = ?$$
$$R(U, S) = 0$$



The Adjoint Method

Background &
Literature Review

Methodology

Results

Conclusions &
Future Work

Publications

References

A.k.a.: Lagrange multipliers, co-state problem, or dual problem.

J : Function of interest. R : Governing equations.

U : State variables (ex: conservative variables).

S : Design variables/independent variables (ex: surface shape).

$$J(U, S) \quad \frac{\delta J}{\delta S} = ?$$

$$R(U, S) = 0$$

$$\delta J = \frac{\partial J}{\partial U} \delta U + \frac{\partial J}{\partial S} \delta S$$

$$\delta R = 0 = \frac{\partial R}{\partial U} \delta U + \frac{\partial R}{\partial S} \delta S$$



The Adjoint Method

Background &
Literature Review

Methodology

Results

Conclusions &
Future Work

Publications

References

A.k.a.: Lagrange multipliers, co-state problem, or dual problem.

J : Function of interest. R : Governing equations.

U : State variables (ex: conservative variables).

S : Design variables/independent variables (ex: surface shape).

$$J(U, S) \quad \frac{\delta J}{\delta S} = ?$$

$$R(U, S) = 0$$

$$\delta J = \frac{\partial J}{\partial U} \delta U + \frac{\partial J}{\partial S} \delta S$$

$$\delta R = 0 = \frac{\partial R}{\partial U} \delta U + \frac{\partial R}{\partial S} \delta S$$

$$\delta \mathcal{J} = \delta J - \psi \delta R = \delta U \left(\frac{\partial J}{\partial U} - \psi \frac{\partial R}{\partial U} \right) + \delta S \left(\frac{\partial J}{\partial S} - \psi \frac{\partial R}{\partial S} \right)$$



The Adjoint Method

Background &
Literature Review

Methodology

Results

Conclusions &
Future Work

Publications

References

A.k.a.: Lagrange multipliers, co-state problem, or dual problem.

J : Function of interest. R : Governing equations.

U : State variables (ex: conservative variables).

S : Design variables/independent variables (ex: surface shape).

$$J(U, S) \quad \frac{\delta J}{\delta S} = ?$$

$$R(U, S) = 0$$

$$\delta J = \frac{\partial J}{\partial U} \delta U + \frac{\partial J}{\partial S} \delta S$$

$$\delta R = 0 = \frac{\partial R}{\partial U} \delta U + \frac{\partial R}{\partial S} \delta S$$

$$\delta \mathcal{J} = \delta J - \psi \delta R = \delta U \left(\frac{\partial J}{\partial U} - \psi \frac{\partial R}{\partial U} \right) + \delta S \left(\frac{\partial J}{\partial S} - \psi \frac{\partial R}{\partial S} \right)$$

$$\text{choose } \psi \text{ s.t. } \left(\frac{\partial J}{\partial U} - \psi \frac{\partial R}{\partial U} \right) = 0$$



The Adjoint Method

Background &
Literature Review

Methodology

Results

Conclusions &
Future Work

Publications

References

A.k.a.: Lagrange multipliers, co-state problem, or dual problem.

J : Function of interest. R : Governing equations.

U : State variables (ex: conservative variables).

S : Design variables/independent variables (ex: surface shape).

$$J(U, S) \quad \frac{\delta J}{\delta S} = ?$$

$$R(U, S) = 0$$

$$\delta J = \frac{\partial J}{\partial U} \delta U + \frac{\partial J}{\partial S} \delta S$$

$$\delta R = 0 = \frac{\partial R}{\partial U} \delta U + \frac{\partial R}{\partial S} \delta S$$

$$\delta \mathcal{J} = \delta J - \psi \delta R = \delta U \left(\frac{\partial J}{\partial U} - \psi \frac{\partial R}{\partial U} \right) + \delta S \left(\frac{\partial J}{\partial S} - \psi \frac{\partial R}{\partial S} \right)$$

$$\text{choose } \psi \text{ s.t. } \left(\frac{\partial J}{\partial U} - \psi \frac{\partial R}{\partial U} \right) = 0$$

$$\rightarrow \frac{\delta J}{\delta S} = \left(\frac{\partial J}{\partial S} - \psi \frac{\partial R}{\partial S} \right)$$



The Continuous Adjoint for Fluid Flow

Background &
Literature Review

Methodology

Results

Conclusions &
Future Work

Publications

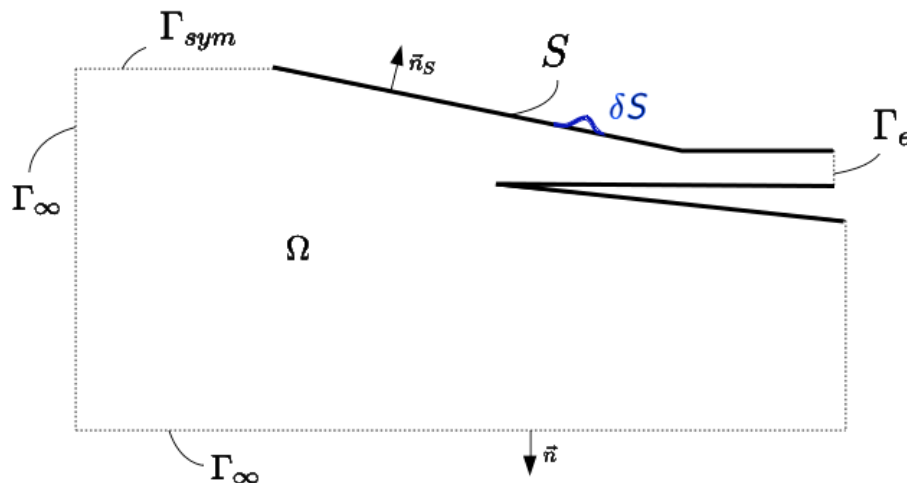
References

$\mathcal{R}(U) = 0$ represents the Euler equations, and the RANS form is included in the thesis.

$$U = \begin{Bmatrix} \rho \\ \rho \vec{v} \\ \rho E \end{Bmatrix}, \Psi = \begin{Bmatrix} \psi_\rho \\ \vec{\varphi} \\ \psi_{\rho E} \end{Bmatrix}, V = \begin{Bmatrix} \rho \\ \vec{v} \\ P \end{Bmatrix}$$

$$\min_S J = \int_{\Gamma_e} j(U) ds$$

subject to: $\mathcal{R}(U) = 0$,





The Continuous Adjoint for Fluid Flow

Background &
Literature Review

Methodology

Results

Conclusions &
Future Work

Publications

References

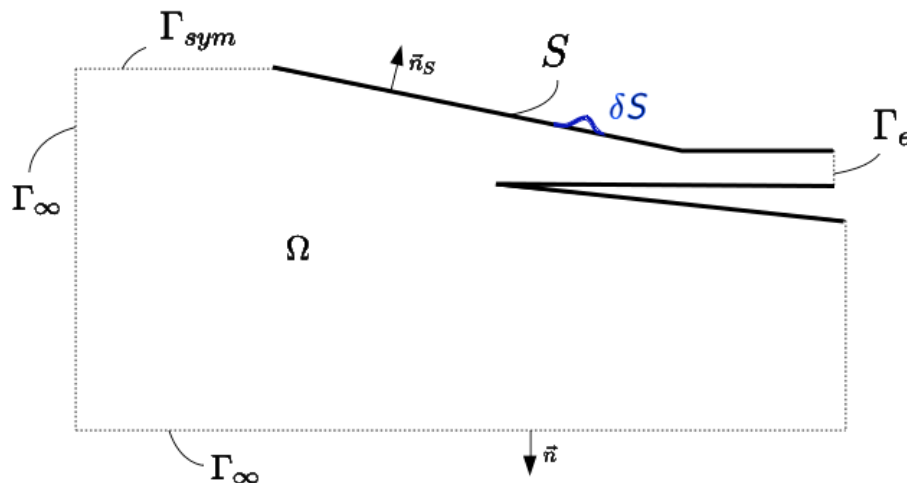
$\mathcal{R}(U) = 0$ represents the Euler equations, and the RANS form is included in the thesis.

$$U = \begin{Bmatrix} \rho \\ \rho \vec{v} \\ \rho E \end{Bmatrix}, \Psi = \begin{Bmatrix} \psi_\rho \\ \vec{\varphi} \\ \psi_{\rho E} \end{Bmatrix}, V = \begin{Bmatrix} \rho \\ \vec{v} \\ P \end{Bmatrix}$$

$$\min_S J = \int_{\Gamma_e} j(U) ds$$

subject to: $\mathcal{R}(U) = 0$,

$$\delta \mathcal{J} = \delta J - \int_{\Omega} \Psi^T \delta \mathcal{R}(U) d\Omega$$





The Continuous Adjoint for Fluid Flow

Background &
Literature Review

Methodology

Results

Conclusions &
Future Work

Publications

References

$\mathcal{R}(U) = 0$ represents the Euler equations, and the RANS form is included in the thesis.

$$U = \begin{Bmatrix} \rho \\ \rho \vec{v} \\ \rho E \end{Bmatrix}, \Psi = \begin{Bmatrix} \psi_\rho \\ \vec{\varphi} \\ \psi_{\rho E} \end{Bmatrix}, V = \begin{Bmatrix} \rho \\ \vec{v} \\ P \end{Bmatrix}$$

$$\min_S J = \int_{\Gamma_e} j(U) ds$$

subject to: $\mathcal{R}(U) = 0$,

$$\delta \mathcal{J} = \delta J - \int_{\Omega} \Psi^T \delta \mathcal{R}(U) d\Omega$$

Find Ψ s.t. $\delta \mathcal{J}$
independent of all unknown
 δU .

$$\delta \mathcal{J} = \int_S \left(\frac{\partial J}{\partial S}(\Psi, U) \right) \delta S ds$$

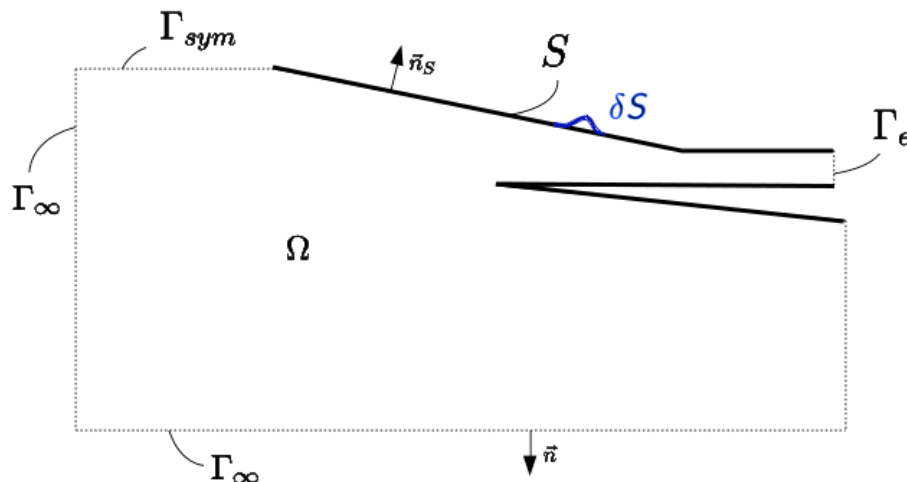




Table of Contents

Background &
Literature Review

Methodology

Results

Conclusions &
Future Work

Publications

References

① Background & Literature Review

② Methodology

- Continuous Adjoint for Generalized Outflow Functional
- Multi-Fidelity Flowpath Linked to Adjoint Sensitivities
- Multi-Objective Adjoint

③ Results

④ Conclusions & Future Work



Continuous Adjoint Method Derivation

Expanding the Lagrangian: $\delta \mathcal{J} = \delta J - \int_{\Omega} \Psi^T \delta \mathcal{R}(U) d\Omega$, with the assumption that Γ_e is undeformed:

Background &
Literature Review

Methodology

Results

Conclusions &
Future Work

Publications

References



Continuous Adjoint Method Derivation

Background &
Literature Review

Methodology

Results

Conclusions &
Future Work

Publications

References

Expanding the Lagrangian: $\delta \mathcal{J} = \delta J - \int_{\Omega} \Psi^T \delta \mathcal{R}(U) d\Omega$, with the assumption that Γ_e is undeformed:

$$\delta J = \int_{\delta \Gamma_e} j(U) ds + \int_{\Gamma_e} \frac{\partial j}{\partial U} \delta U ds = \int_{\Gamma_e} j(U) ds - \int_{\Gamma_e} j(U) ds + \int_{\Gamma_e} \frac{\partial j}{\partial U} \delta U ds = \int_{\Gamma_e} \frac{\partial j}{\partial U} \delta U ds$$



Continuous Adjoint Method Derivation

Background &
Literature Review

Methodology

Results

Conclusions &
Future Work

Publications

References

Expanding the Lagrangian: $\delta \mathcal{J} = \delta J - \int_{\Omega} \Psi^T \delta \mathcal{R}(U) d\Omega$, with the assumption that Γ_e is undeformed:

$$\delta J = \int_{\delta \Gamma_e} j(U) ds + \int_{\Gamma_e} \frac{\partial j}{\partial U} \delta U ds = \int_{\Gamma_e} j(U) ds - \int_{\Gamma_e} j(U) ds + \int_{\Gamma_e} \frac{\partial j}{\partial U} \delta U ds = \int_{\Gamma_e} \frac{\partial j}{\partial U} \delta U ds$$

Applying the divergence theorem to the second term:

$$\int_{\Omega} \Psi^T \delta \mathcal{R}(U) d\Omega = \int_{\Gamma} \Psi^T \vec{A} \cdot \vec{n} \delta U ds + \int_S \Psi^T \vec{A} \cdot \vec{n} \delta U ds + \int_S \Psi^T \vec{A} \cdot \vec{n} \delta S ds - \int_{\Omega} \nabla \Psi^T \vec{A} \delta U d\Omega$$



Continuous Adjoint Method Derivation

Background &
Literature Review

Methodology

Results

Conclusions &
Future Work

Publications

References

Expanding the Lagrangian: $\delta \mathcal{J} = \delta J - \int_{\Omega} \Psi^T \delta \mathcal{R}(U) d\Omega$, with the assumption that Γ_e is undeformed:

$$\delta J = \int_{\delta \Gamma_e} j(U) ds + \int_{\Gamma_e} \frac{\partial j}{\partial U} \delta U ds = \int_{\Gamma_e} j(U) ds - \int_{\Gamma_e} j(U) ds + \int_{\Gamma_e} \frac{\partial j}{\partial U} \delta U ds = \int_{\Gamma_e} \frac{\partial j}{\partial U} \delta U ds$$

Applying the divergence theorem to the second term:

$$\int_{\Omega} \Psi^T \delta \mathcal{R}(U) d\Omega = \int_{\Gamma} \Psi^T \vec{A} \cdot \vec{n} \delta U ds + \int_S \Psi^T \vec{A} \cdot \vec{n} \delta U ds + \int_S \Psi^T \vec{A} \cdot \vec{n} \delta S ds - \int_{\Omega} \nabla \Psi^T \vec{A} \delta U d\Omega$$

Combining the terms above:

$$\begin{aligned} \delta \mathcal{J} = & \int_{\Gamma_e} \frac{\partial j}{\partial U} \delta U ds - \int_{\Gamma} \Psi^T \vec{A} \cdot \vec{n} \delta U ds - \int_S \Psi^T \vec{A} \cdot \vec{n} \delta U ds \\ & - \int_S \Psi^T \vec{A} \cdot \vec{n} U \delta S ds + \int_{\Omega} \nabla \Psi^T \cdot \vec{A} \delta U d\Omega \end{aligned}$$



Continuous Adjoint Method Derivation

Background &
Literature Review

Methodology

Results

Conclusions &
Future Work

Publications

References

Expanding the Lagrangian: $\delta \mathcal{J} = \delta J - \int_{\Omega} \Psi^T \delta \mathcal{R}(U) d\Omega$, with the assumption that Γ_e is undeformed:

$$\delta J = \int_{\delta \Gamma_e} j(U) ds + \int_{\Gamma_e} \frac{\partial j}{\partial U} \delta U ds = \int_{\Gamma_e} j(U) ds - \int_{\Gamma_e} j(U) ds + \int_{\Gamma_e} \frac{\partial j}{\partial U} \delta U ds = \int_{\Gamma_e} \frac{\partial j}{\partial U} \delta U ds$$

Applying the divergence theorem to the second term:

$$\int_{\Omega} \Psi^T \delta \mathcal{R}(U) d\Omega = \int_{\Gamma} \Psi^T \vec{A} \cdot \vec{n} \delta U ds + \int_S \Psi^T \vec{A} \cdot \vec{n} \delta U ds + \int_S \Psi^T \vec{A} \cdot \vec{n} \delta S ds - \int_{\Omega} \nabla \Psi^T \vec{A} \delta U d\Omega$$

Combining the terms above:

Terms that lead to boundary conditions

$$\delta \mathcal{J} = \int_{\Gamma_e} \frac{\partial j}{\partial U} \delta U ds - \int_{\Gamma} \Psi^T \vec{A} \cdot \vec{n} \delta U ds - \int_S \Psi^T \vec{A} \cdot \vec{n} \delta U ds - \int_S \Psi^T \vec{A} \cdot \vec{n} U \delta S ds + \int_{\Omega} \nabla \Psi^T \cdot \vec{A} \delta U d\Omega$$



Continuous Adjoint Method Derivation

Background &
Literature Review

Methodology

Results

Conclusions &
Future Work

Publications

References

Expanding the Lagrangian: $\delta \mathcal{J} = \delta J - \int_{\Omega} \Psi^T \delta \mathcal{R}(U) d\Omega$, with the assumption that Γ_e is undeformed:

$$\delta J = \int_{\delta \Gamma_e} j(U) ds + \int_{\Gamma_e} \frac{\partial j}{\partial U} \delta U ds = \int_{\Gamma_e} j(U) ds - \int_{\Gamma_e} j(U) ds + \int_{\Gamma_e} \frac{\partial j}{\partial U} \delta U ds = \int_{\Gamma_e} \frac{\partial j}{\partial U} \delta U ds$$

Applying the divergence theorem to the second term:

$$\int_{\Omega} \Psi^T \delta \mathcal{R}(U) d\Omega = \int_{\Gamma} \Psi^T \vec{A} \cdot \vec{n} \delta U ds + \int_S \Psi^T \vec{A} \cdot \vec{n} \delta U ds + \int_S \Psi^T \vec{A} \cdot \vec{n} \delta S ds - \int_{\Omega} \nabla \Psi^T \vec{A} \delta U d\Omega$$

Combining the terms above:

$$\delta \mathcal{J} = \int_{\Gamma_e} \frac{\partial j}{\partial U} \delta U ds - \int_{\Gamma} \Psi^T \vec{A} \cdot \vec{n} \delta U ds - \int_S \Psi^T \vec{A} \cdot \vec{n} \delta U ds - \int_S \Psi^T \vec{A} \cdot \vec{n} U \delta S ds + \int_{\Omega} \nabla \Psi^T \cdot \vec{A} \delta U d\Omega$$

Terms that lead to surface sensitivity



Continuous Adjoint Method Derivation

Background &
Literature Review

Methodology

Results

Conclusions &
Future Work

Publications

References

Expanding the Lagrangian: $\delta \mathcal{J} = \delta J - \int_{\Omega} \Psi^T \delta \mathcal{R}(U) d\Omega$, with the assumption that Γ_e is undeformed:

$$\delta J = \int_{\delta \Gamma_e} j(U) ds + \int_{\Gamma_e} \frac{\partial j}{\partial U} \delta U ds = \int_{\Gamma_e} j(U) ds - \int_{\Gamma_e} j(U) ds + \int_{\Gamma_e} \frac{\partial j}{\partial U} \delta U ds = \int_{\Gamma_e} \frac{\partial j}{\partial U} \delta U ds$$

Applying the divergence theorem to the second term:

$$\int_{\Omega} \Psi^T \delta \mathcal{R}(U) d\Omega = \int_{\Gamma} \Psi^T \vec{A} \cdot \vec{n} \delta U ds + \int_S \Psi^T \vec{A} \cdot \vec{n} \delta U ds + \int_S \Psi^T \vec{A} \cdot \vec{n} \delta S ds - \int_{\Omega} \nabla \Psi^T \vec{A} \delta U d\Omega$$

Combining the terms above:

$$\delta \mathcal{J} = \int_{\Gamma_e} \frac{\partial j}{\partial U} \delta U ds - \int_{\Gamma} \Psi^T \vec{A} \cdot \vec{n} \delta U ds - \int_S \Psi^T \vec{A} \cdot \vec{n} \delta U ds - \int_S \Psi^T \vec{A} \cdot \vec{n} U \delta S ds + \int_{\Omega} \nabla \Psi^T \cdot \vec{A} \delta U d\Omega$$

Terms that lead to the adjoint governing equation



Continuous Adjoint Method Derivation

Background &
Literature Review

Methodology

Results

Conclusions &
Future Work

Publications

References

Expanding the Lagrangian: $\delta \mathcal{J} = \delta J - \int_{\Omega} \Psi^T \delta \mathcal{R}(U) d\Omega$, with the assumption that Γ_e is undeformed:

$$\delta J = \int_{\delta \Gamma_e} j(U) ds + \int_{\Gamma_e} \frac{\partial j}{\partial U} \delta U ds = \int_{\cancel{\Gamma_e}} j(U) ds - \int_{\cancel{\Gamma_e}} j(U) ds + \int_{\Gamma_e} \frac{\partial j}{\partial U} \delta U ds = \int_{\Gamma_e} \frac{\partial j}{\partial U} \delta U ds$$

Applying the divergence theorem to the second term:

$$\int_{\Omega} \Psi^T \delta \mathcal{R}(U) d\Omega = \int_{\Gamma} \Psi^T \vec{A} \cdot \vec{n} \delta U ds + \int_S \Psi^T \vec{A} \cdot \vec{n} \delta U ds + \int_S \Psi^T \vec{A} \cdot \vec{n} \delta S ds - \int_{\Omega} \nabla \Psi^T \vec{A} \delta U d\Omega$$

Combining the terms above:

$$\delta \mathcal{J} = \int_{\Gamma_e} \frac{\partial j}{\partial U} \delta U ds - \int_{\Gamma} \Psi^T \vec{A} \cdot \vec{n} \delta U ds - \int_S \Psi^T \vec{A} \cdot \vec{n} \delta U ds - \int_S \Psi^T \vec{A} \cdot \vec{n} U \delta S ds + \int_{\Omega} \nabla \Psi^T \cdot \vec{A} \delta U d\Omega$$

Remaining terms are similar to (Castro et al. 2007); terms are simplified using differential geometry, integration by parts, and the linearized form of the direct problem boundary conditions.



Generalized Outflow Boundary Conditions

We need to make $\frac{\partial j}{\partial U} \delta U - \Psi^T \vec{A} \cdot \vec{n} \delta U$ independent of δU .

Background &
Literature Review

Methodology

Results

Conclusions &
Future Work

Publications

References



Generalized Outflow Boundary Conditions

We need to make $\frac{\partial j}{\partial V} \delta V - \Psi^T \vec{A} \cdot \vec{n} M \delta V$ independent of δV .

Background &
Literature Review

Methodology

Results

Conclusions &
Future Work

Publications

References



Generalized Outflow Boundary Conditions

We need to make $\frac{\partial j}{\partial V} \delta V - \Psi^T \vec{A} \cdot \vec{n} M \delta V$ independent of δV . When expanded, this equation is:

$$\begin{Bmatrix} \frac{\partial j}{\partial \rho} \\ \frac{\partial j}{\partial \vec{v}} \\ \frac{\partial j}{\partial P} \end{Bmatrix}^T \begin{Bmatrix} \delta \rho \\ \delta \vec{v} \\ \delta P \end{Bmatrix} - \begin{Bmatrix} \psi_\rho v_n + \vec{v} \cdot \vec{\varphi} v_n + \psi_{\rho E} v_n \left(\frac{v^2}{2} \right) \\ \rho (\vec{v} \cdot \vec{\varphi}) \vec{n} + \rho v_n \vec{\varphi} + \rho \psi_\rho \vec{n} + \psi_{\rho E} \left(\rho v_n \vec{v} + \rho \left(\frac{c^2}{\gamma-1} + \gamma \frac{v^2}{2} \right) \vec{n} \right) \\ \vec{\varphi} \cdot \vec{n} + \psi_{\rho E} \left(v_n \frac{\gamma}{\gamma-1} \right) \end{Bmatrix}^T \begin{Bmatrix} \delta \rho \\ \delta \vec{v} \\ \delta P \end{Bmatrix}$$



Generalized Outflow Boundary Conditions

We need to make $\frac{\partial j}{\partial V} \delta V - \Psi^T \vec{A} \cdot \vec{n} M \delta V$ independent of δV . When expanded, this equation is:

$$\begin{Bmatrix} \frac{\partial j}{\partial \rho} \\ \frac{\partial j}{\partial \vec{v}} \\ \frac{\partial j}{\partial P} \end{Bmatrix}^T \begin{Bmatrix} \delta \rho \\ \delta \vec{v} \\ \delta P \end{Bmatrix} - \begin{Bmatrix} \psi_\rho v_n + \vec{v} \cdot \vec{\varphi} v_n + \psi_{\rho E} v_n \left(\frac{v^2}{2} \right) \\ \rho (\vec{v} \cdot \vec{\varphi}) \vec{n} + \rho v_n \vec{\varphi} + \rho \psi_\rho \vec{n} + \psi_{\rho E} \left(\rho v_n \vec{v} + \rho \left(\frac{c^2}{\gamma-1} + \gamma \frac{v^2}{2} \right) \vec{n} \right) \\ \vec{\varphi} \cdot \vec{n} + \psi_{\rho E} \left(v_n \frac{\gamma}{\gamma-1} \right) \end{Bmatrix}^T \begin{Bmatrix} \delta \rho \\ \delta \vec{v} \\ \delta P \end{Bmatrix}$$

When flow is subsonic and a constant pressure condition is used, $\delta P = 0$. In order to eliminate dependence on the remaining $\delta \rho$ and $\delta \vec{v}$:

$$\begin{Bmatrix} \psi_\rho \\ \vec{\varphi} \end{Bmatrix} = \psi_{\rho E} \begin{Bmatrix} \frac{2c^2 + v^2(\gamma-1)}{2(\gamma-1)} \\ -\vec{n} \frac{c^2}{v_n(\gamma-1)} - \vec{v} \end{Bmatrix} + \begin{Bmatrix} - \left(\frac{\partial j}{\partial \vec{v}} \cdot \vec{v} \frac{1}{\rho v_n} \right) + \left(\frac{\partial j}{\partial \rho} \frac{2}{v_n} \right) \\ \left(\frac{\partial j}{\partial \vec{v}} \frac{1}{\rho v_n} - \vec{n} \frac{\partial j}{\partial \rho} \frac{1}{v_n^2} \right) \end{Bmatrix}$$



Generalized Outflow Boundary Conditions

We need to make $\frac{\partial j}{\partial V} \delta V - \Psi^T \vec{A} \cdot \vec{n} M \delta V$ independent of δV . When expanded, this equation is:

$$\begin{Bmatrix} \frac{\partial j}{\partial \rho} \\ \frac{\partial j}{\partial \vec{v}} \\ \frac{\partial j}{\partial P} \end{Bmatrix}^T \begin{Bmatrix} \delta \rho \\ \delta \vec{v} \\ \delta P \end{Bmatrix} - \begin{Bmatrix} \psi_\rho v_n + \vec{v} \cdot \vec{\varphi} v_n + \psi_{\rho E} v_n \left(\frac{v^2}{2} \right) \\ \rho (\vec{v} \cdot \vec{\varphi}) \vec{n} + \rho v_n \vec{\varphi} + \rho \psi_\rho \vec{n} + \psi_{\rho E} \left(\rho v_n \vec{v} + \rho \left(\frac{c^2}{\gamma-1} + \gamma \frac{v^2}{2} \right) \vec{n} \right) \\ \vec{\varphi} \cdot \vec{n} + \psi_{\rho E} \left(v_n \frac{\gamma}{\gamma-1} \right) \end{Bmatrix}^T \begin{Bmatrix} \delta \rho \\ \delta \vec{v} \\ \delta P \end{Bmatrix}$$

When flow is subsonic and a constant pressure condition is used, $\delta P = 0$. In order to eliminate dependence on the remaining $\delta \rho$ and $\delta \vec{v}$:

$$\begin{Bmatrix} \psi_\rho \\ \vec{\varphi} \end{Bmatrix} = \psi_{\rho E} \begin{Bmatrix} \frac{2c^2 + v^2(\gamma-1)}{2(\gamma-1)} \\ -\vec{n} \frac{c^2}{v_n(\gamma-1)} - \vec{v} \end{Bmatrix} + \begin{Bmatrix} - \left(\frac{\partial j}{\partial \vec{v}} \cdot \vec{v} \frac{1}{\rho v_n} \right) + \left(\frac{\partial j}{\partial \rho} \frac{2}{v_n} \right) \\ \left(\frac{\partial j}{\partial \vec{v}} \frac{1}{\rho v_n} - \vec{n} \frac{\partial j}{\partial \rho} \frac{1}{v_n^2} \right) \end{Bmatrix}$$

When the flow is supersonic, the dependence on δP is eliminated through:

$$\psi_{\rho E, M > 1} = \frac{\gamma-1}{v_n^2 - c^2} \left(\frac{\partial j}{\partial \rho} \frac{1}{v_n} + \frac{\partial j}{\partial P} v_n - \frac{\partial j}{\partial \vec{v}} \cdot \vec{n} \frac{1}{\rho} \right)$$



Generalized Outflow Boundary Conditions

We need to make $\frac{\partial j}{\partial V} \delta V - \Psi^T \vec{A} \cdot \vec{n} M \delta V$ independent of δV . When expanded, this equation is:

$$\begin{Bmatrix} \frac{\partial j}{\partial \rho} \\ \frac{\partial j}{\partial \vec{v}} \\ \frac{\partial j}{\partial P} \end{Bmatrix}^T \begin{Bmatrix} \delta \rho \\ \delta \vec{v} \\ \delta P \end{Bmatrix} - \begin{Bmatrix} \psi_\rho v_n + \vec{v} \cdot \vec{\varphi} v_n + \psi_{\rho E} v_n \left(\frac{v^2}{2} \right) \\ \rho (\vec{v} \cdot \vec{\varphi}) \vec{n} + \rho v_n \vec{\varphi} + \rho \psi_\rho \vec{n} + \psi_{\rho E} \left(\rho v_n \vec{v} + \rho \left(\frac{c^2}{\gamma-1} + \gamma \frac{v^2}{2} \right) \vec{n} \right) \\ \vec{\varphi} \cdot \vec{n} + \psi_{\rho E} \left(v_n \frac{\gamma}{\gamma-1} \right) \end{Bmatrix}^T \begin{Bmatrix} \delta \rho \\ \delta \vec{v} \\ \delta P \end{Bmatrix}$$

When flow is subsonic and a constant pressure condition is used, $\delta P = 0$. In order to eliminate dependence on the remaining $\delta \rho$ and $\delta \vec{v}$:

$$\begin{Bmatrix} \psi_\rho \\ \vec{\varphi} \end{Bmatrix} = \psi_{\rho E} \begin{Bmatrix} \frac{2c^2 + v^2(\gamma-1)}{2(\gamma-1)} \\ -\vec{n} \frac{c^2}{v_n(\gamma-1)} - \vec{v} \end{Bmatrix} + \begin{Bmatrix} - \left(\frac{\partial j}{\partial \vec{v}} \cdot \vec{v} \frac{1}{\rho v_n} \right) + \left(\frac{\partial j}{\partial \rho} \frac{2}{v_n} \right) \\ \left(\frac{\partial j}{\partial \vec{v}} \frac{1}{\rho v_n} - \vec{n} \frac{\partial j}{\partial \rho} \frac{1}{v_n^2} \right) \end{Bmatrix}$$

When the flow is supersonic, the dependence on δP is eliminated through:

$$\psi_{\rho E, M > 1} = \frac{\gamma-1}{v_n^2 - c^2} \left(\frac{\partial j}{\partial \rho} \frac{1}{v_n} + \frac{\partial j}{\partial P} v_n - \frac{\partial j}{\partial \vec{v}} \cdot \vec{n} \frac{1}{\rho} \right)$$



Multi-Fidelity Flowpath

Background &
Literature Review

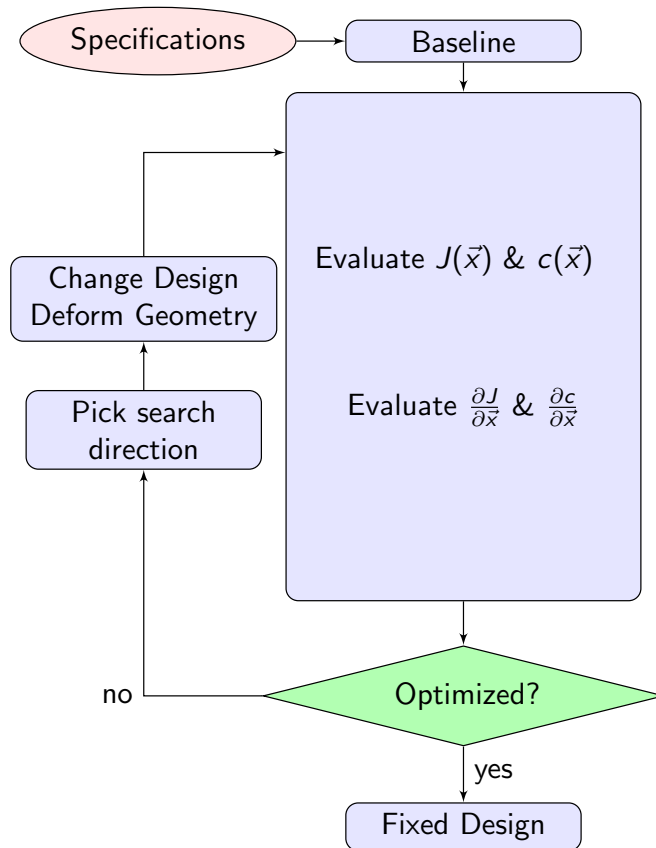
Methodology

Results

Conclusions &
Future Work

Publications

References





Multi-Fidelity Flowpath

Background &
Literature Review

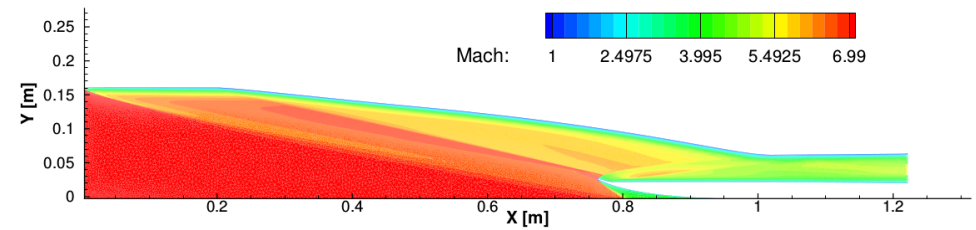
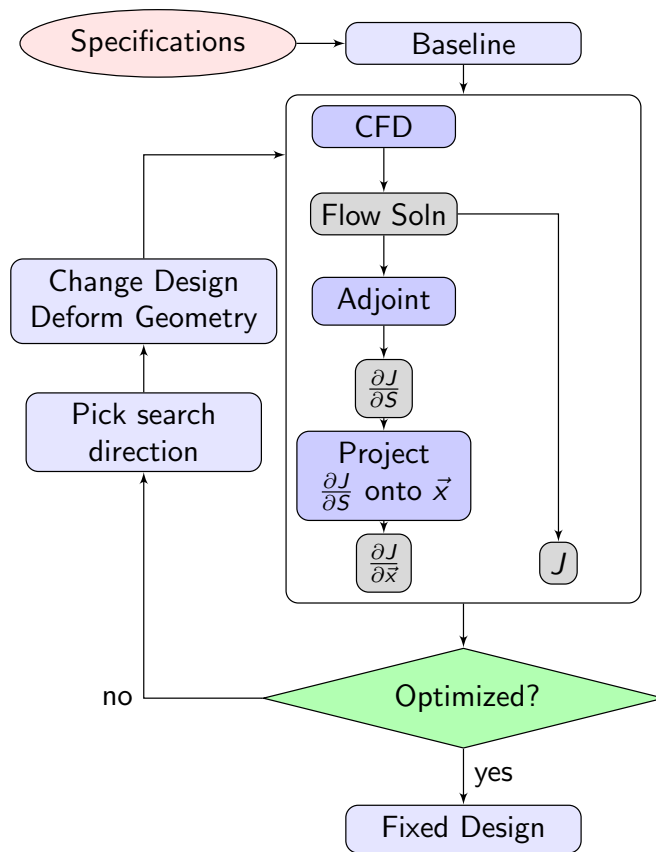
Methodology

Results

Conclusions &
Future Work

Publications

References



Mach 7 flow through 2D scramjet inlet.



Multi-Fidelity Flowpath

Background & Literature Review

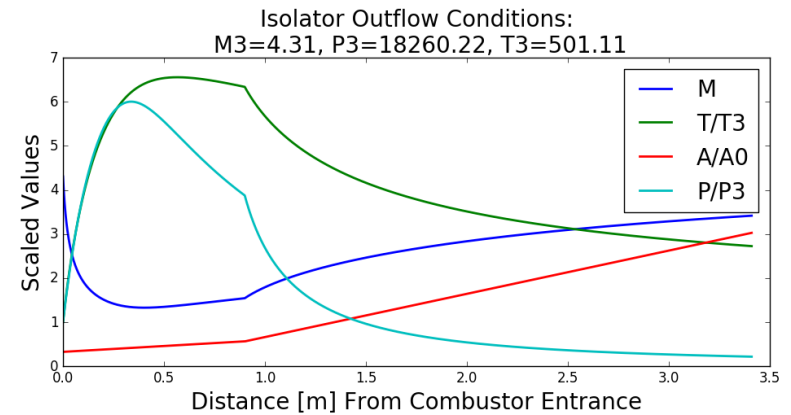
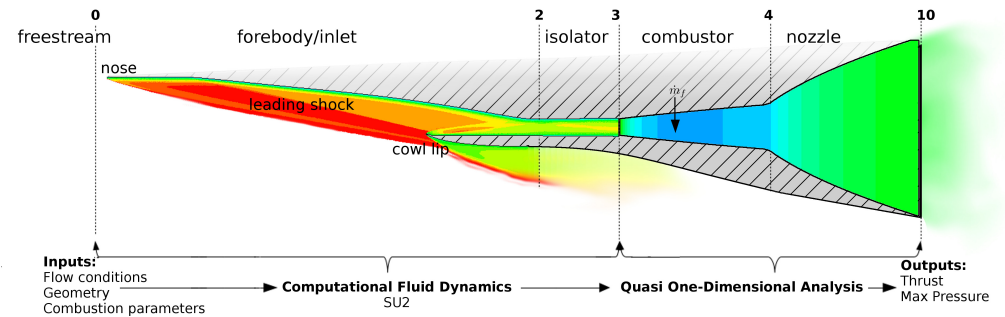
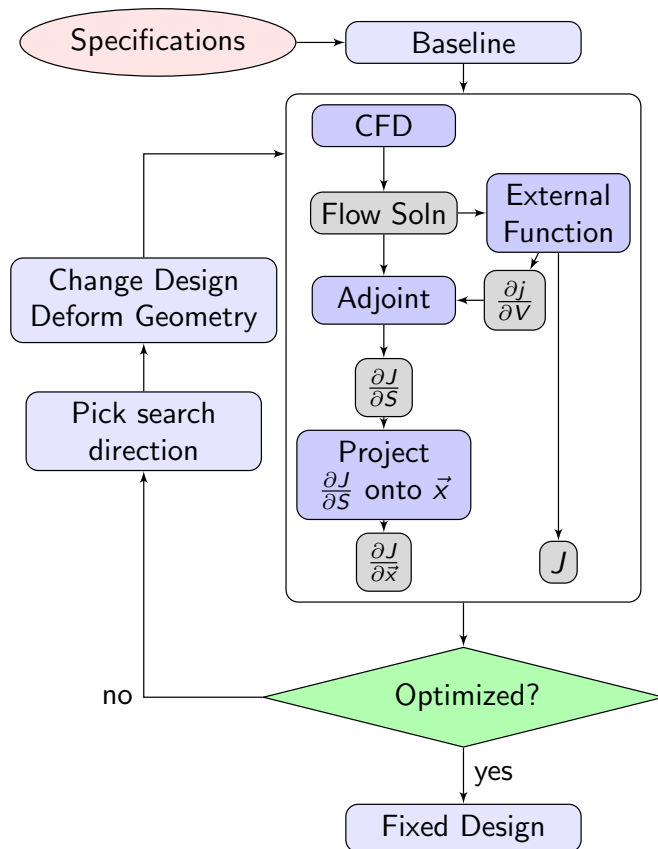
Methodology

Results

Conclusions & Future Work

Publications

References



Example output from combustion model & expansion model. Conditions match initial geometry and Mach 7 flow.



One-Dimensionalization Methods

Any method of one-dimensionalization will necessarily lose some information about the flow. Multiple methods exist, each of which have pros and cons.

$$J = f(\bar{V})$$
$$\delta J = \frac{\partial J}{\partial \bar{V}} \int_{\Gamma} \frac{\partial \bar{V}}{\partial V} \delta V ds$$
$$\frac{\partial j}{\partial V} = \frac{\partial J}{\partial \bar{V}} \frac{\partial \bar{V}}{\partial V}$$

Area-Averaging

$$\bar{V} = \left\{ \begin{array}{l} \int \rho ds \\ \int v_n ds \\ \int P ds \end{array} \right\} \frac{1}{\mathcal{A}_e}$$

$$\frac{\partial \bar{V}}{\partial V} = \frac{1}{\mathcal{A}_e} \left\{ \begin{array}{l} 1, \quad 0, \quad 0 \\ \vec{0}, \quad \vec{n}, \quad \vec{0} \\ 0, \quad 0, \quad 1 \end{array} \right\}$$



One-Dimensionalization Methods

Background &
Literature Review

Methodology

Results

Conclusions &
Future Work

Publications

References

Any method of one-dimensionalization will necessarily lose some information about the flow. Multiple methods exist, each of which have pros and cons.

$$J = f(\bar{V})$$

$$\delta J = \frac{\partial J}{\partial \bar{V}} \int_{\Gamma} \frac{\partial \bar{V}}{\partial V} \delta V ds$$

$$\frac{\partial j}{\partial V} = \frac{\partial J}{\partial \bar{V}} \frac{\partial \bar{V}}{\partial V}$$

Mass-Flux Averaging

$$\bar{V} = \left\{ \begin{array}{l} \frac{\int \rho(v_n) ds / \dot{m}}{\sqrt{(\int v_n^2 (\rho v_n) ds / \dot{m})}} \\ \int P(\rho v_n) ds / \dot{m} \end{array} \right\}$$

$$\frac{\partial \bar{V}}{\partial V} = \left\{ \begin{array}{lll} v_n (2\rho - \bar{\rho}), & \frac{v_n (v_n^2 - \bar{v}^2)}{2\bar{v}}, & v_n (P - \bar{P}) \\ \rho \vec{n} (\rho - \bar{\rho}), & \frac{\rho (v_n \vec{v} + |\vec{v}|^2 \vec{n} - \bar{v}^2 \vec{n})}{2\bar{v}}, & \rho \vec{n} (P - \bar{P}) \\ 0, & 0, & \rho v_n \end{array} \right\} \frac{1}{\dot{m}}$$



Verification of Implemented Methods

Background & Literature Review

Methodology

Results

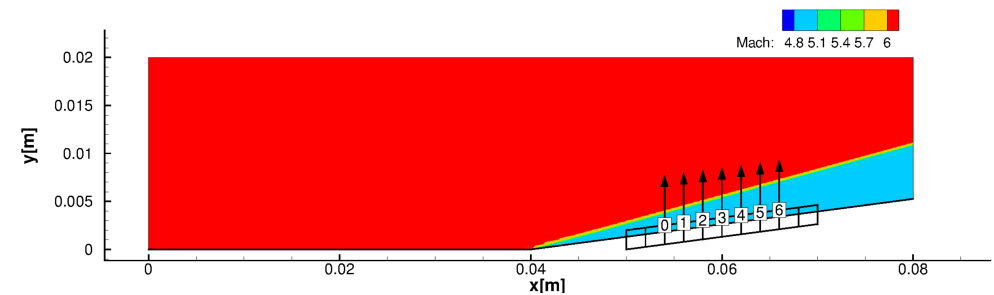
Conclusions & Future Work

Publications

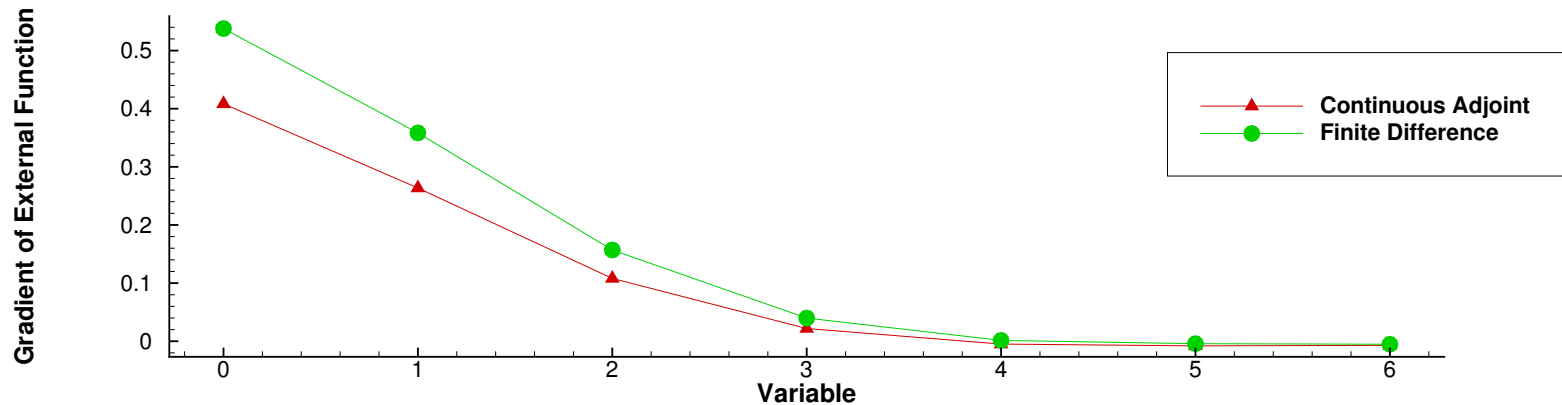
References

Verification test case: scaled specific installed thrust, evaluated using values at the outflow boundary of a ramp in Mach 6 flow. Results shown are for area averaged method.

$$J = \frac{\mathcal{F}_{un} - D_{est}}{2000\dot{m}}$$



Test geometry and variables.



Gradient of specific installed thrust computed in an external script.



Multi-Objective Adjoint Implementation

Background &
Literature Review

Methodology

Results

Conclusions &
Future Work

Publications

References

Multi-objective adjoint evaluation can be obtained by utilizing the principle of superposition for linear PDEs:

$$\delta(w_1 J_1 + w_2 J_2) = w_1 \delta J_1 + w_2 \delta J_2.$$

- Re-uses existing functionals, requiring care with scaling factors.
- Also possible to evaluate the sensitivity of constraints defined as a penalty function of existing functionals via the chain rule.

$$\delta(J_1 + f(J_2)) = \delta J_1 + \frac{\partial f}{\partial J_2} \delta J_2.$$



Multi-Objective Adjoint Implementation

Background &
Literature Review

Methodology

Results

Conclusions &
Future Work

Publications

References

Multi-objective adjoint evaluation can be obtained by utilizing the principle of superposition for linear PDEs:

$$\delta(w_1 J_1 + w_2 J_2) = w_1 \delta J_1 + w_2 \delta J_2.$$

- Re-uses existing functionals, requiring care with scaling factors.
- Also possible to evaluate the sensitivity of constraints defined as a penalty function of existing functionals via the chain rule.

$$\delta(J_1 + f(J_2)) = \delta J_1 + \frac{\partial f}{\partial J_2} \delta J_2.$$

Var.	$\frac{\partial(C_D \times 10^5 + \bar{P}_t \times 10^{-5})}{\partial x_i}$ (simultaneous)	$\frac{\partial C_D}{\partial x_i} \times 10^5 + \frac{\bar{P}_t}{\partial x_i} \times 10^{-5}$ (separate)
0	-1.50232998E+2	-1.50232998E+2
1	-9.40390906E+1	-9.40390906E+1
2	-4.40948556E+1	-4.40948556E+1
3	-1.58777572E+1	-1.58777572E+1
4	-4.30593276E+0	-4.30593276E+0
5	-7.47768208E-1	-7.47768208E-1
6	8.61790879E-2	8.61790874E-2



Generalizations of the Continuous Adjoint Method

Background &
Literature Review

Methodology

Results

Conclusions &
Future Work

Publications

References

- Derived & implemented the adjoint for a generalized outflow-based functional, and implemented multi-fidelity flowpath to provide partial derivative values.

$$J = \int_{\Gamma_e} j(V) ds, \quad V = \{\rho, \vec{v}^T, P\}^T$$

$$\begin{Bmatrix} \psi_\rho \\ \vec{\varphi} \end{Bmatrix} = \psi_{\rho E} \begin{Bmatrix} \frac{2c^2 + \vec{v}^2(\gamma-1)}{2(\gamma-1)} \\ -\vec{n} \frac{c^2}{v_n(\gamma-1)} - \vec{v} \end{Bmatrix} + \begin{Bmatrix} -\left(\frac{\partial j}{\partial \vec{v}} \cdot \vec{v} \frac{1}{\rho v_n}\right) + \left(\frac{\partial j}{\partial \rho} \frac{2}{v_n}\right) \\ \left(\frac{\partial j}{\partial \vec{v}} \frac{1}{\rho v_n} - \vec{n} \frac{\partial j}{\partial \rho} \frac{1}{v_n^2}\right) \end{Bmatrix}$$

$$\psi_{\rho E, M>1} = \frac{\gamma-1}{v_n^2 - c^2} \left(\frac{\partial j}{\partial \rho} \frac{1}{v_n} + \frac{\partial j}{\partial P} v_n - \frac{\partial j}{\partial \vec{v}} \cdot \vec{n} \frac{1}{\rho} \right)$$

- Multi-objective adjoint evaluation utilizing the principle of superposition for linear PDEs & re-utilizing existing boundary conditions.
- Implemented in the open-source simulation suite SU2¹.

¹T. Economon et al. (2016). "SU2 : An Open-Source Suite for Multiphysics Simulation and Design". In: [AIAA Journal](#) 54.3, pp. 828–846.



Table of Contents

Background &
Literature Review

Methodology

Results

Conclusions &
Future Work

Publications

References

① Background & Literature Review

② Methodology

③ Results

- Initial Point Design
- 2D Optimization & Comparisons of Sensitivity
- 3D Optimization With Penalty Function

④ Conclusions & Future Work



Initial Point Design

Background &
Literature Review

Methodology

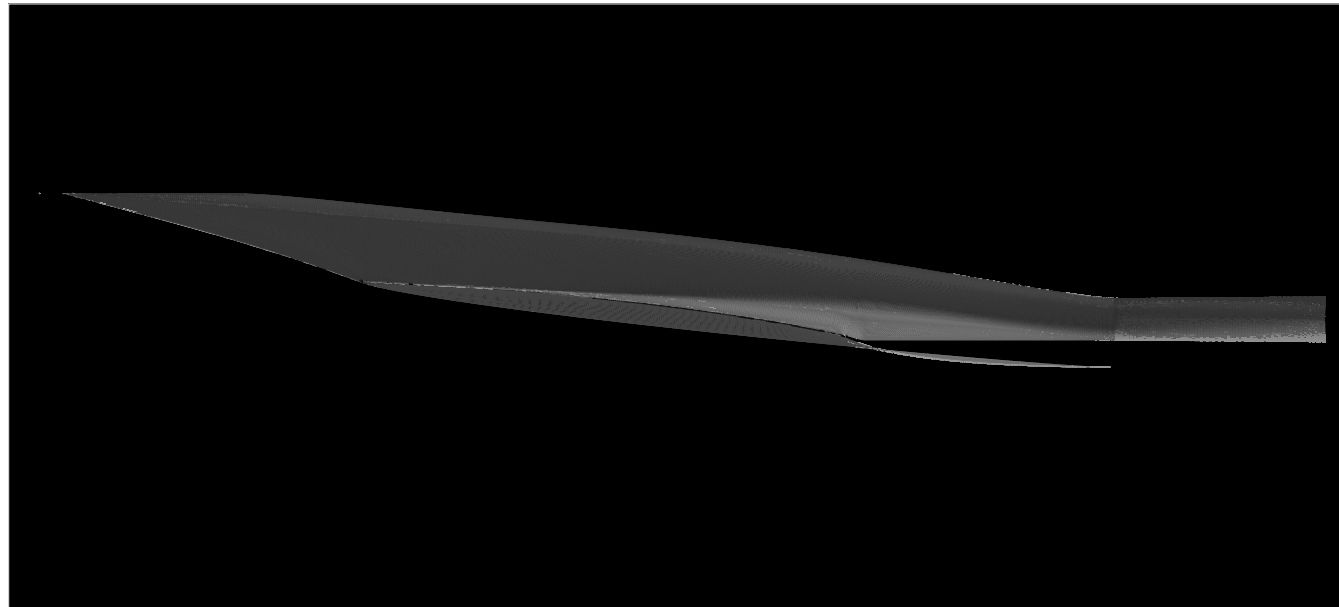
Results

Conclusions &
Future Work

Publications

References

Initial geometry: Rectangular-to-Elliptical-Shape-Transition (REST) inlet¹ in Mach 7 flow with dynamic pressure of 82 kPa, Re of 6×10^6 .



¹P. G. Ferlemann and R. J. Gollan (2010). "Parametric Geometry, Structured Grid Generation, and Initial Design Study for REST-Class Hypersonic Inlets". In:



Initial Point Design

Background & Literature Review

Methodology

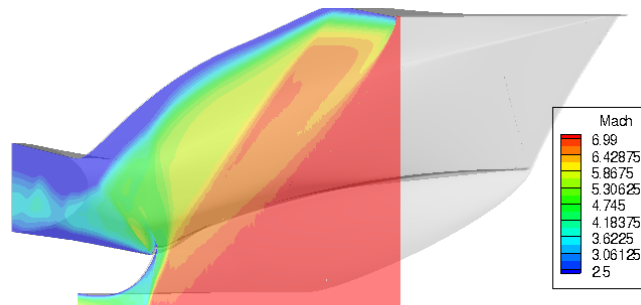
Results

Conclusions & Future Work

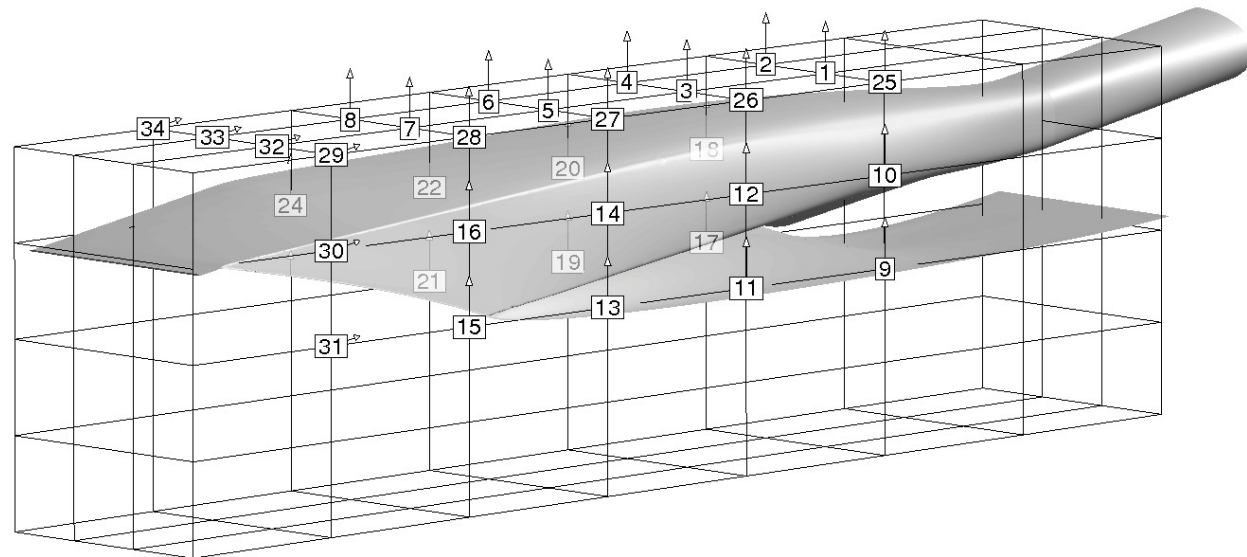
Publications

References

Initial geometry: Rectangular-to-Elliptical-Shape-Transition (REST) inlet¹ in Mach 7 flow with dynamic pressure of 82 kPa, Re of 6×10^6 .



Shape design variables are Free-Form-Deformation (FFD) points.



¹P. G. Ferlemann and R. J. Gollan (2010). "Parametric Geometry, Structured Grid Generation, and Initial Design Study for REST-Class Hypersonic Inlets". In:



Initial 2D Optimization Problem

Background &
Literature Review

Methodology

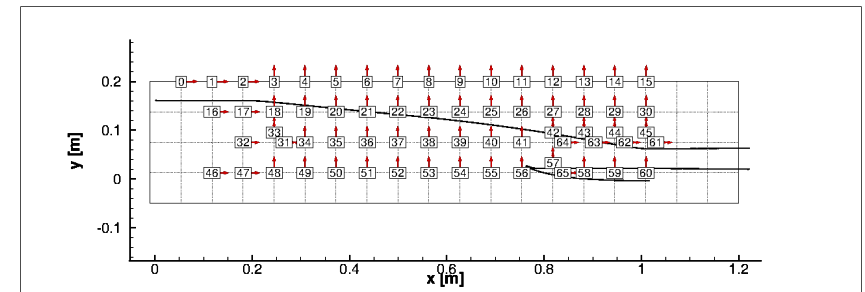
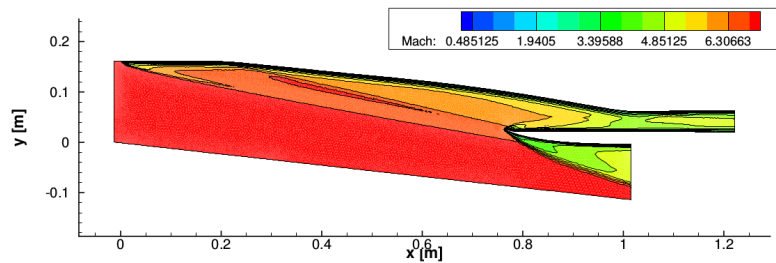
Results

Conclusions &
Future Work

Publications

References

Symmetry plane of the same 3-dimensional
Rectangular-to-Elliptical-Shape-Transition (REST) inlet¹.



Non-Linear Program (NLP):

$$\min_{\vec{x}} J(\vec{x})$$

$$\text{subject to: } \vec{x}_l \leq \vec{x} \leq \vec{x}_u,$$

$$c_j(\vec{x}) < 0$$

$$J = -P_{t3}$$

(total pressure)

$$J = -\frac{F_{un} - D_{est}}{\dot{m}}$$

(specific installed thrust)

$$J = -\frac{F_{un} - D_{est}}{\dot{m}} + 10^2 (\max(\tau_e - \tau_{lim}, 0.0))^2$$

("with total temperature penalty")

$$J = -\frac{F_{un} - D_{est}}{\dot{m}} + 10^2 \left(\max\left(\frac{\tau_e - \tau_{lim}}{\tau_{lim}}, 0.0\right) \right)^4 + 10^5 \left(\max\left(\frac{P_{max} - P_{lim}}{P_{lim}}, 0.0\right) \right)^4$$

("with max pressure penalty")

¹P. G. Ferlemann and R. J. Gollan (2010). "Parametric Geometry, Structured Grid Generation, and Initial Design Study for REST-Class Hypersonic Inlets". In:



Initial 2D Optimization Problem

Background & Literature Review

Methodology

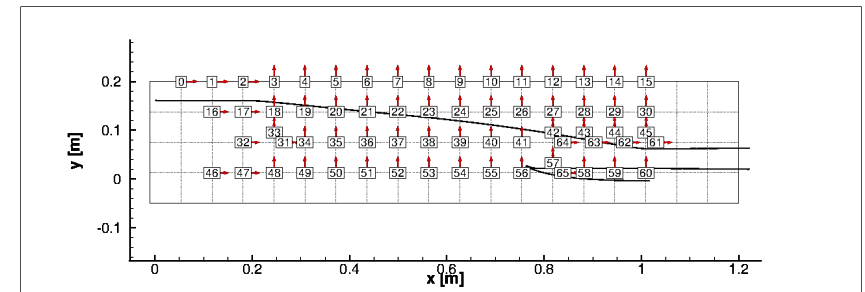
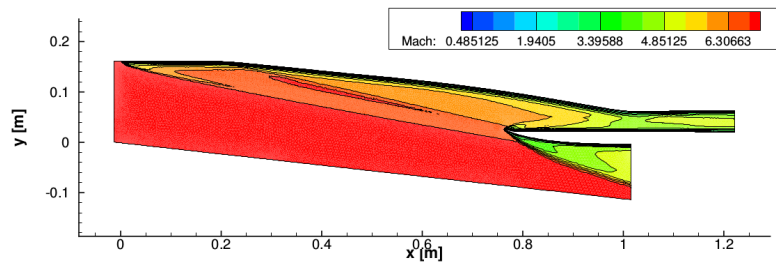
Results

Conclusions & Future Work

Publications

References

Symmetry plane of the same 3-dimensional Rectangular-to-Elliptical-Shape-Transition (REST) inlet¹.



Non-Linear Program (NLP):

$$\min_{\vec{x}} J(\vec{x}) + \text{Penalty}(c_j(\vec{x}))$$

$$\text{subject to: } \vec{x}_l \leq \vec{x} \leq \vec{x}_u,$$

$$J = -P_{t3}$$

(total pressure)

$$J = -\frac{F_{un} - D_{est}}{\dot{m}}$$

(specific installed thrust)

$$J = -\frac{F_{un} - D_{est}}{\dot{m}} + 10^2 (\max(\tau_e - \tau_{lim}, 0.0))^2$$

("with total temperature penalty")

$$J = -\frac{F_{un} - D_{est}}{\dot{m}} + 10^2 \left(\max\left(\frac{\tau_e - \tau_{lim}}{\tau_{lim}}, 0.0\right) \right)^4 + 10^5 \left(\max\left(\frac{P_{max} - P_{lim}}{P_{lim}}, 0.0\right) \right)^4$$

("with max pressure penalty")

¹P. G. Ferlemann and R. J. Gollan (2010). "Parametric Geometry, Structured Grid Generation, and Initial Design Study for REST-Class Hypersonic Inlets". In:



Initial 2D Optimization Problem

Background & Literature Review

Methodology

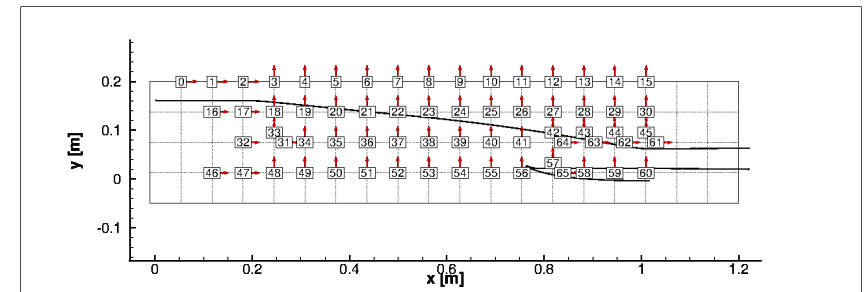
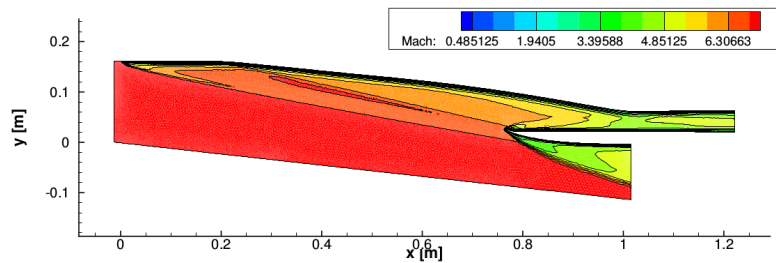
Results

Conclusions & Future Work

Publications

References

Symmetry plane of the same 3-dimensional Rectangular-to-Elliptical-Shape-Transition (REST) inlet¹.



Non-Linear Program (NLP):

$$\min_{\vec{x}} J(\vec{x}) + \text{Penalty}(c_j(\vec{x}))$$

$$\text{subject to: } \vec{x}_l \leq \vec{x} \leq \vec{x}_u,$$

$$J = -P_{t3}$$

(total pressure)

$$J = -\frac{F_{un} - D_{est}}{\dot{m}}$$

(specific installed thrust)

$$J = -\frac{F_{un} - D_{est}}{\dot{m}} + 10^2 (\max(\tau_e - \tau_{lim}, 0.0))^2$$

("with total temperature penalty")

$$J = -\frac{F_{un} - D_{est}}{\dot{m}} + 10^2 \left(\max\left(\frac{\tau_e - \tau_{lim}}{\tau_{lim}}, 0.0\right) \right)^4 + 10^5 \left(\max\left(\frac{P_{max} - P_{lim}}{P_{lim}}, 0.0\right) \right)^4$$

("with max pressure penalty")

¹P. G. Ferlemann and R. J. Gollan (2010). "Parametric Geometry, Structured Grid Generation, and Initial Design Study for REST-Class Hypersonic Inlets". In:



Sensitivity Comparisons

Background &
Literature Review

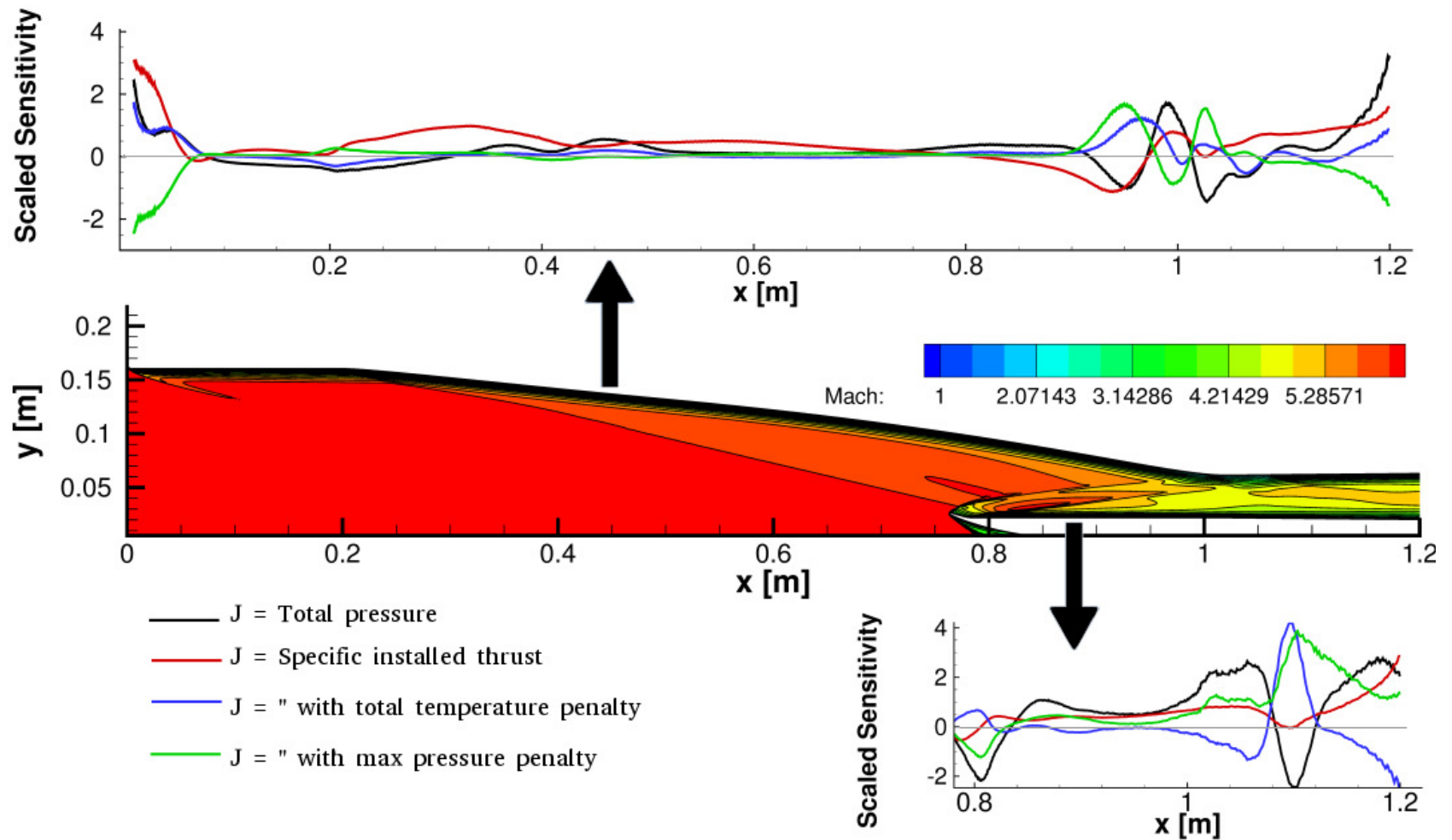
Methodology

Results

Conclusions &
Future Work

Publications

References



Surface sensitivity on the ramp and cowl surfaces for a 2D simulation of the symmetry plane. Sensitivities are scaled by the integrated norm of the sensitivity.



2D Optimization Results

Background &
Literature Review

Methodology

Results

Conclusions &
Future Work

Publications

References

Objective Function	P_{t3}	$\frac{F_{un-Dest}}{\dot{m}}$	\dot{m}	τ_e	P_{max}
$J = -P_{t3}$ (total pressure)	+1.86%	-0.57%	+0.29%	-0.08%	+1.32%
$J = -\frac{F_{un-Dest}}{\dot{m}}$ (specific installed thrust)	+6.54%	+17.08%	+1.09%	+0.07%	+0.06%
$J = -\frac{F_{un-Dest}}{\dot{m}}$ $+10^2 (\max(\tau_e - \tau_{lim}, 0.0))^2$ (" with total temperature penalty)	-2.54%	+24.47%	+2.22%	-0.20%	+1.72%
$J = -\frac{F_{un-Dest}}{\dot{m}}$ $+10^2 \left(\max \left(\frac{\tau_e - \tau_{lim}}{\tau_{lim}}, 0.0 \right) \right)^4$ $+10^5 \left(\max \left(\frac{P_{max} - P_{lim}}{P_{lim}}, 0.0 \right) \right)^4$ (" with max pressure penalty)	+0.45%	-10.00%	-0.92%	+0.10%	-0.94%



2D Optimization Results

- Background & Literature Review
- Methodology
- Results
- Conclusions & Future Work
- Publications
- References

Objective Function	P_{t3}	$\frac{F_{un-Dest}}{\dot{m}}$	\dot{m}	τ_e	P_{max}
$J = -P_{t3}$ (total pressure)	+1.86%	-0.57%	+0.29%	-0.08%	+1.32%
$J = -\frac{F_{un-Dest}}{\dot{m}}$ (specific installed thrust)	+6.54%	+17.08%	+1.09%	+0.07%	+0.06%
$J = -\frac{F_{un-Dest}}{\dot{m}}$ $+10^2 (\max(\tau_e - \tau_{lim}, 0.0))^2$ (" with total temperature penalty)	-2.54%	+24.47%	+2.22%	-0.20%	+1.72%
$J = -\frac{F_{un-Dest}}{\dot{m}}$ $+10^2 \left(\max\left(\frac{\tau_e - \tau_{lim}}{\tau_{lim}}, 0.0\right) \right)^4$ $+10^5 \left(\max\left(\frac{P_{max} - P_{lim}}{P_{lim}}, 0.0\right) \right)^4$ (" with max pressure penalty)	+0.45%	-10.00%	-0.92%	+0.10%	-0.94%



2D Optimization Results

Background &
Literature Review

Methodology

Results

Conclusions &
Future Work

Publications

References

Objective Function	P_{t3}	$\frac{F_{un-Dest}}{\dot{m}}$	\dot{m}	τ_e	P_{max}
$J = -P_{t3}$ (total pressure)	+1.86%	-0.57%	+0.29%	-0.08%	+1.32%
$J = -\frac{F_{un-Dest}}{\dot{m}}$ (specific installed thrust)	+6.54%	+17.08%	+1.09%	+0.07%	+0.06%
$J = -\frac{F_{un-Dest}}{\dot{m}}$ $+10^2 (\max(\tau_e - \tau_{lim}, 0.0))^2$ (" with total temperature penalty)	-2.54%	+24.47%	+2.22%	-0.20%	+1.72%
$J = -\frac{F_{un-Dest}}{\dot{m}}$ $+10^2 \left(\max \left(\frac{\tau_e - \tau_{lim}}{\tau_{lim}}, 0.0 \right) \right)^4$ $+10^5 \left(\max \left(\frac{P_{max} - P_{lim}}{P_{lim}}, 0.0 \right) \right)^4$ (" with max pressure penalty)	+0.45%	-10.00%	-0.92%	+0.10%	-0.94%



2D Optimization Results

Background &
Literature Review

Methodology

Results

Conclusions &
Future Work

Publications

References

Objective Function	P_{t3}	$\frac{F_{un-Dest}}{\dot{m}}$	\dot{m}	τ_e	P_{max}
$J = -P_{t3}$ (total pressure)	+1.86%	-0.57%	+0.29%	-0.08%	+1.32%
$J = -\frac{F_{un-Dest}}{\dot{m}}$ (specific installed thrust)	+6.54%	+17.08%	+1.09%	+0.07%	+0.06%
$J = -\frac{F_{un-Dest}}{\dot{m}}$ $+10^2 (\max(\tau_e - \tau_{lim}, 0.0))^2$ (" with total temperature penalty)	-2.54%	+24.47%	+2.22%	-0.20%	+1.72%
$J = -\frac{F_{un-Dest}}{\dot{m}}$ $+10^2 \left(\max\left(\frac{\tau_e - \tau_{lim}}{\tau_{lim}}, 0.0\right) \right)^4$ $+10^5 \left(\max\left(\frac{P_{max} - P_{lim}}{P_{lim}}, 0.0\right) \right)^4$ (" with max pressure penalty)	+0.45%	-10.00%	-0.92%	+0.10%	-0.94%



2D Optimization Results

Background &
Literature Review

Methodology

Results

Conclusions &
Future Work

Publications

References

Objective Function	P_{t3}	$\frac{F_{un}-D_{est}}{\dot{m}}$	\dot{m}	τ_e	P_{max}
$J = -P_{t3}$ (total pressure)	+1.86%	-0.57%	+0.29%	-0.08%	+1.32%
$J = -\frac{F_{un}-D_{est}}{\dot{m}}$ (specific installed thrust)	+6.54%	+17.08%	+1.09%	+0.07%	+0.06%
$J = -\frac{F_{un}-D_{est}}{\dot{m}}$ $+10^2 (\max(\tau_e - \tau_{lim}, 0.0))^2$ (" with total temperature penalty)	-2.54%	+24.47%	+2.22%	-0.20%	+1.72%
$J = -\frac{F_{un}-D_{est}}{\dot{m}}$ $+10^2 \left(\max \left(\frac{\tau_e - \tau_{lim}}{\tau_{lim}}, 0.0 \right) \right)^4$ $+10^5 \left(\max \left(\frac{P_{max} - P_{lim}}{P_{lim}}, 0.0 \right) \right)^4$ (" with max pressure penalty)	+0.45%	-10.00%	-0.92%	+0.10%	-0.94%



2D Optimization Results

- Background & Literature Review
- Methodology
- Results
- Conclusions & Future Work
- Publications
- References

Objective Function	P_{t3}	$\frac{F_{un-Dest}}{\dot{m}}$	\dot{m}	τ_e	P_{max}
$J = -P_{t3}$ (total pressure)	+1.86%	-0.57%	+0.29%	-0.08%	+1.32%
$J = -\frac{F_{un-Dest}}{\dot{m}}$ (specific installed thrust)	+6.54%	+17.08%	+1.09%	+0.07%	+0.06%
$J = -\frac{F_{un-Dest}}{\dot{m}}$ $+10^2 (\max(\tau_e - \tau_{lim}, 0.0))^2$ (" with total temperature penalty)	-2.54%	+24.47%	+2.22%	-0.20%	+1.72%
$J = -\frac{F_{un-Dest}}{\dot{m}}$ $+10^2 \left(\max \left(\frac{\tau_e - \tau_{lim}}{\tau_{lim}}, 0.0 \right) \right)^4$ $+10^5 \left(\max \left(\frac{P_{max} - P_{lim}}{P_{lim}}, 0.0 \right) \right)^4$ (" with max pressure penalty)	+0.45%	-10.00%	-0.92%	+0.10%	-0.94%



3D Optimization Problem Statement

Background & Literature Review

Methodology

Results

Conclusions & Future Work

Publications

References

Non-Linear Program for the 3D case:

$$\min_{\vec{x}} J(\vec{x}) = -\frac{\mathcal{F}_{un} - D_{est}}{\dot{m}}$$

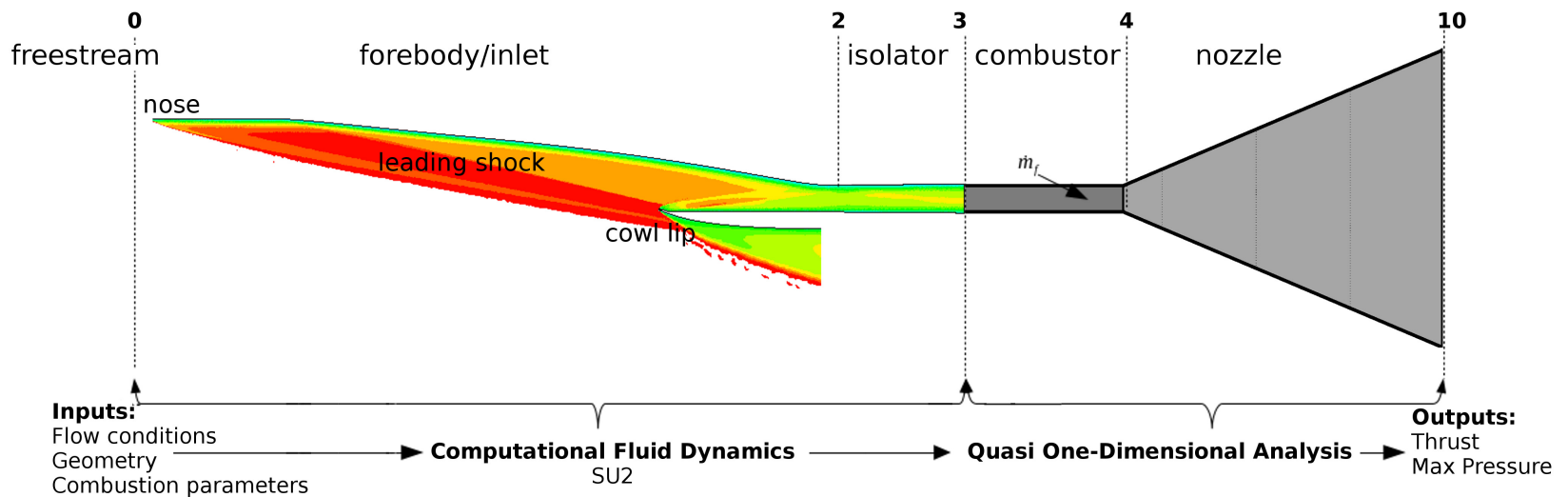
subject to: $\vec{x}_l \leq \vec{x} \leq \vec{x}_u$,

$$IHF \leq IHF_{lim}$$

$$P_{max} \leq P_{lim}$$

$$\tau_e \leq \tau_{lim}$$

$IHF = \int -k \nabla T ds$ is the Integrated Heat Flux over the wetted surfaces included in the CFD volume.





3D Optimization Problem Statement

Background & Literature Review

Methodology

Results

Conclusions & Future Work

Publications

References

Non-Linear Program for the 3D case:

$$\min_{\vec{x}} J(\vec{x}) = -\frac{\mathcal{F}_{un} - D_{est}}{\dot{m}}$$

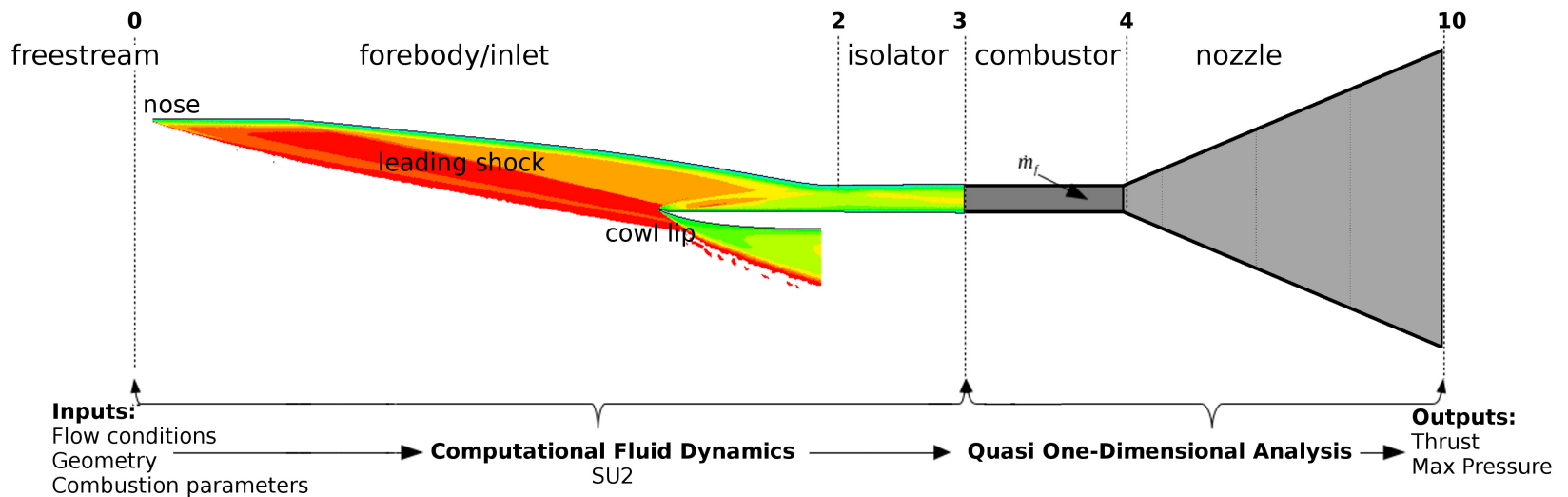
subject to: $\vec{x}_l \leq \vec{x} \leq \vec{x}_u$,

$$IHF \leq IHF_{lim}$$

$$P_{max} \leq P_{lim}$$

$$\tau_e \leq \tau_{lim}$$

$IHF = \int -k \nabla T ds$ is the Integrated Heat Flux over the wetted surfaces included in the CFD volume.





3D Optimization Problem Statement

Background & Literature Review

Methodology

Results

Conclusions & Future Work

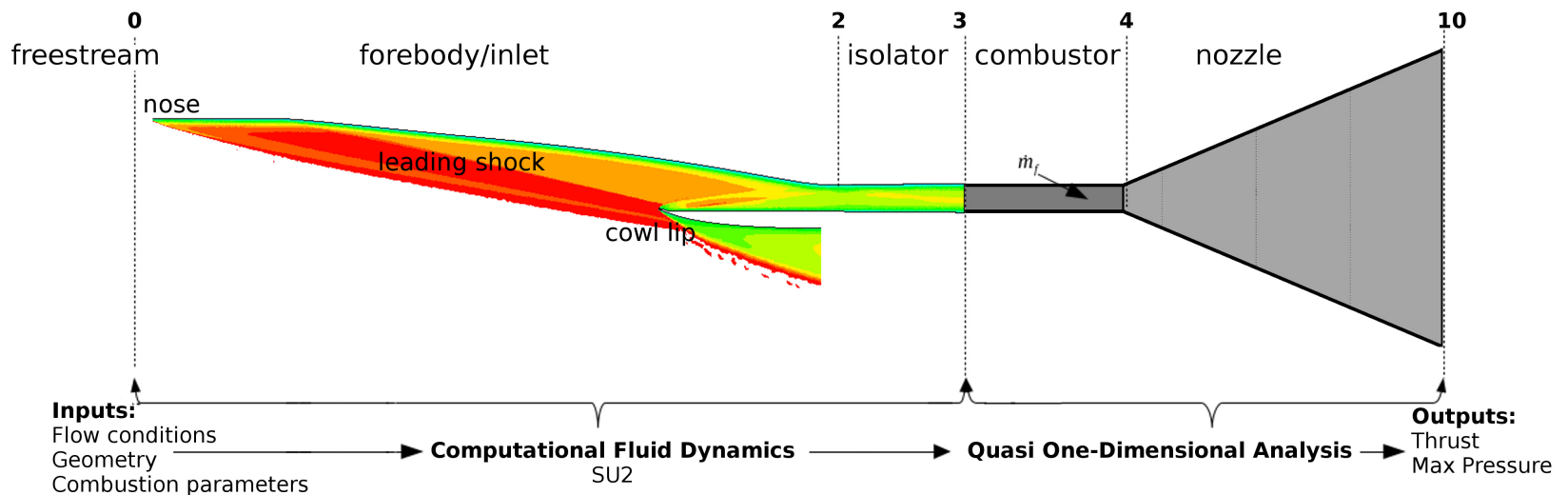
Publications

References

Non-Linear Program for the 3D case:

$$\begin{aligned} \min_{\vec{x}} J'(\vec{x}) = & -\frac{\mathcal{F}_{un} - D_{est}}{\dot{m}} \\ & + 10^{-5} (\max(IHF - IHF_{lim}, 0.0))^2 \\ & + 10^{-5} (\max(P_{max} - P_{lim}, 0.0))^2 \\ & + 10^5 (\max(\tau_e - \tau_{lim}, 0.0))^2 \end{aligned}$$

$IHF = \int -k \nabla T ds$ is the Integrated Heat Flux over the wetted surfaces included in the CFD volume.





Three-Dimensional Optimization Results

Background & Literature Review

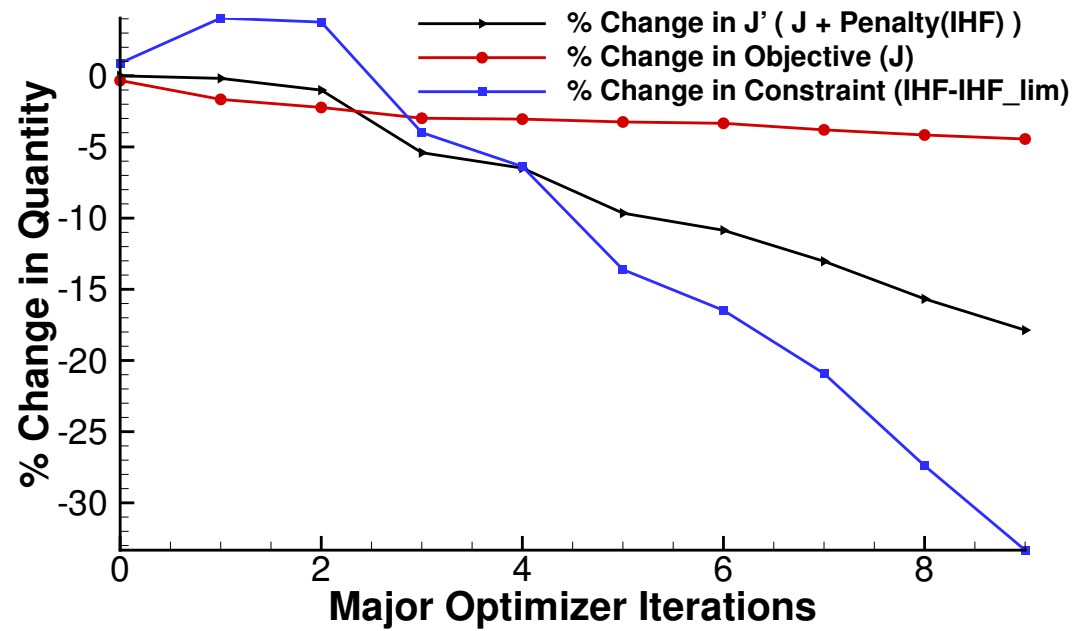
Methodology

Results

Conclusions & Future Work

Publications

References



Change in performance metrics						
J'	$\frac{\mathcal{F}_{un-Dest}}{\dot{m}}$	P_{t3}	\dot{m}	$IHF - IHF_{lim}$	τ_e	P_{max}
-17.9%	+4.10%	-0.194%	+0.206%	-33.9%	-2E - 3%	+0.11%



Three-Dimensional Optimization Results

Background &
Literature Review

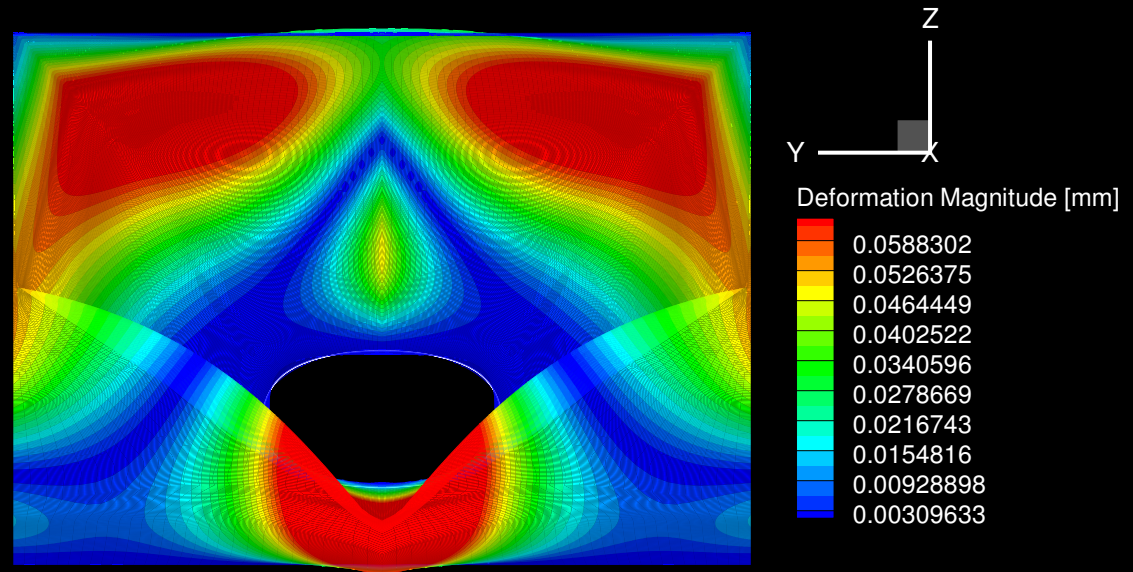
Methodology

Results

Conclusions &
Future Work

Publications

References



Deformation Visualization Exaggerated x100

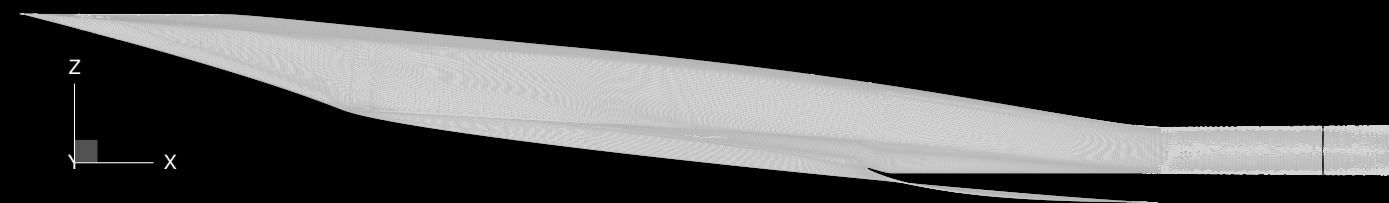




Table of Contents

Background &
Literature Review

Methodology

Results

Conclusions &
Future Work

Publications

References

① Background & Literature Review

② Methodology

③ Results

④ Conclusions & Future Work



Contributions

Background &
Literature Review

Methodology

Results

Conclusions &
Future Work

Publications

References



Contributions

Background &
Literature Review

Methodology

Results

Conclusions &
Future Work

Publications

References

- A new generalized functional adjoint was derived & implemented, which facilitates **flexible outflow-based functionals**, including those that use **external models**.



Contributions

Background &
Literature Review

Methodology

Results

Conclusions &
Future Work

Publications

References

- A new generalized functional adjoint was derived & implemented, which facilitates **flexible outflow-based functionals**, including those that use **external models**.
- **Multi-objective adjoint** implemented by using superposition of boundary conditions.



Contributions

Background &
Literature Review

Methodology

Results

Conclusions &
Future Work

Publications

References

- A new generalized functional adjoint was derived & implemented, which facilitates **flexible outflow-based functionals**, including those that use **external models**.
- **Multi-objective adjoint** implemented by using superposition of boundary conditions.
- These methods have been implemented in SU2, and utilized for multi-objective and multi-fidelity shape optimization of a hypersonic inlet.



Contributions

Background &
Literature Review

Methodology

Results

Conclusions &
Future Work

Publications

References

- A new generalized functional adjoint was derived & implemented, which facilitates **flexible outflow-based functionals**, including those that use **external models**.
- **Multi-objective adjoint** implemented by using superposition of boundary conditions.
- These methods have been implemented in SU2, and utilized for multi-objective and multi-fidelity shape optimization of a hypersonic inlet.
- These methods provide access to surface sensitivity for more realistic & relevant functionals, for applications including optimization, error estimation, uncertainty quantification, and mesh refinement.



Conclusions & Future Work

Background &
Literature Review

Methodology

Results

Conclusions &
Future Work

Publications

References

Conclusions

- Performance of the inlet is extremely sensitive to small shape deformations.
- Sensitivity plots show correlation between several metrics near the nose, while those metrics have opposing sensitivity within the isolator.
- Optimizing using these methods produces significant improvement in and successfully balances performance metrics.

Potential Further Applications & Extensions

- Application to alternate design problems.
- Generalized objectives on additional boundary types.
- Further studies with more detailed models of the combustor and nozzle.



Publications

Background &
Literature Review

Methodology

Results

Conclusions &
Future Work

Publications

References

- H. Kline, F. Palacios, and J. Alonso (2014). “Sensitivity of the Performance of a 3-Dimensional Hypersonic Inlet to Shape Deformations”. In: [19th AIAA International Space Planes and Hypersonic Systems and Technologies Conference](#). Atlanta, GA
- H. Kline et al. (2015). “Adjoint-Based Optimization of a Hypersonic Inlet”. In: [22nd AIAA Computational Fluid Dynamics Conference](#). Dallas, TX
- H. Kline, T. Economou, and J. Alonso (2016). “Multi-Objective Optimization of a Hypersonic Inlet Using Generalized Outflow Boundary Conditions in the Continuous Adjoint Method”. In: [54th AIAA Aerospace Sciences Meeting](#)
- R. Sanchez et al. (2016b). “Towards a Fluid-Structure Interaction solver for problems with large deformations within the open-source SU2 suite”. In: [57th AIAA/ASCE/AHS/ASC Structures, Structural Dynamics, and Materials Conference](#), p. 0205
- R. Sanchez et al. (2016a). “Assessment Of The Fluid-Structure Interaction Capabilities For Aeronautical Applications Of The Open-Source Solver SU2.” In: [Eccomas congress 2016](#)
- Under Review: AIAA Journal paper, titled “Adjoint of Generalized Outflow-Based Functionals Applied To Hypersonic Inlet Design”

Additional optimization studies omitted from presentation: Pareto fronts of heat flux vs specific installed thrust, 2D 'constrained' optimization (similar to 3D case shown).



Acknowledgements

Background &
Literature Review

Methodology

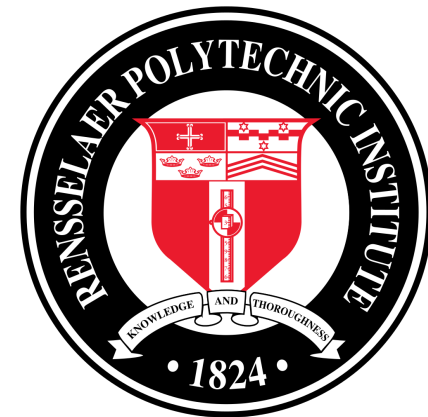
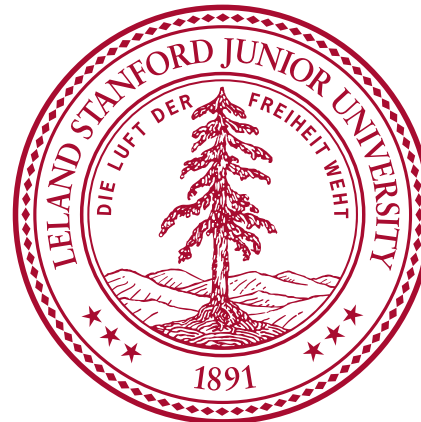
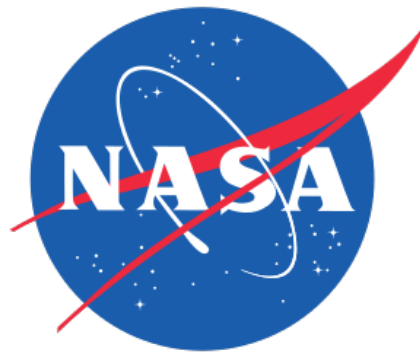
Results

Conclusions &
Future Work

Publications

References

This work was supported by a NASA Space Technology Research Fellowship, grant number NNX12AN23H. This work used the Extreme Science and Engineering Discover Environment (XSEDE), which is supported by National Science Foundation grant number ACI-1053575¹. The first year of graduate study was supported by the Stanford Graduate Fellowship.



I would also like to thank Professor Alonso, the ADL, the SU2 development team, the Hypersonic Airbreathing Propulsion Branch of NASA Langley, Shelly Ferlemann, and my friends and family for their support.

¹J. Towns et al. (2014). "XSEDE: Accelerating Scientific Discovery". In: [Computing in Science & Engineering 16.5](#), pp. 62–74.